Department of Otorhinolaryngology
University of Helsinki
Finland

Auditory cortical processing

Binaural interaction in healthy and *ROBO1*-deficient subjects

Satu Lamminmäki

Brain Research Unit
O.V. Lounasmaa Laboratory
School of Science
Aalto University
Finland

ACADEMIC DISSERTATION

To be presented, by the permission of the Faculty of Medicine of the University of Helsinki, for public examination in the Auditorium S1, Otakaari 5A, at the Aalto University School of Science (Espoo, Finland) on 23rd of November 2012, at 12 noon.

Helsinki 2012

ISBN 978-952-10-8293-1 (printed)
ISBN 978-952-10-8294-8 (pdf)
Unigrafia Oy
Helsinki 2012, Finland

The dissertation can be read at http://ethesis.helsinki.fi

Supervisor:

Academy Professor Riitta Hari
Brain Research Unit
O.V. Lounasmaa Laboratory
School of Science
Aalto University
Finland

Reviewers:

Professor Juhani Partanen
Department of Clinical Neurophysiology
Helsinki University Central Hospital
Finland

Docent Juha-Pekka Vasama
Department of Otorhinolaryngology
Tampere University Hospital
Finland

Official opponent:

Professor Stephanie Clarke
University Hospital and University of Lausanne
Switzerland

Acknowledgements

[Available only in the printed form.]

Contents

List of publications **1**

Abbreviations **3**

Abstract **5**

1 Introduction **7**

2 Review of literature **9**

2.1 Basic anatomy and physiology of the auditory system 9
2.1.1 The outer and middle ear 10
2.1.2 The inner ear 11
2.1.3 Brain stem and thalamus 11
2.1.4 Cortical structures 13

2.2 Binaural interaction in the auditory system 18
2.2.1 Anatomical basis and physiological mechanisms 18
2.2.2 Peculiar binaural processing: The octave illusion 19

2.3 Human *ROBO1* gene and bilateral neurodevelopment 21
2.3.1 *ROBO1* and developmental dyslexia 21

2.4 Magnetoencephalography 23
2.4.1 Physiological basis of MEG signals 23
2.4.2 MEG in the study of auditory processing 25

3 Aims of the study **33**

4 Materials and methods **35**

4.1 Subjects 35
4.1.1 *ROBO1*–deficient dyslexic subjects 36
4.1.2 Hearing levels 36
4.1.3 Psychophysical tests 36

4.2 MEG recordings 37
4.2.1 Stimulation 37
4.2.2 Recordings 37
4.2.3 Data analysis 39
4.3 Genetic tests 40

5 Experiments 41

5.1 Binaural interaction is abnormal in individuals with a *ROBO1* gene defect (Study I) 41
5.1.1 Results 42
5.1.2 Discussion 43
5.2 Auditory transient responses to dichotic tones follow the sound localization during the octave illusion (Study II) 44
5.2.1 Results 44
5.2.2 Discussion 45
5.3 Modified binaural interaction contributes to the peculiar pitch perception during the octave illusion (Study III) 46
5.3.1 Results 46
5.3.2 Discussion 47
5.4 Early cortical processing of natural sounds can be studied with amplitude-modulated speech and music (Study IV) 48
5.4.1 Results 48
5.4.2 Discussion 49

6 General discussion 51

6.1 Connections between *ROBO1*, binaural processing, crossing of auditory pathways, and dyslexia 51
6.2 Binaural processing in the octave illusion 55
6.3 Natural stimuli in studying early cortical processing and binaural interaction 58
6.4 Binaural interaction: clinical aspects 60

7 Conclusion 61

References 63

List of publications

This thesis is based on the following publications:

I. **Lamminmäki S**, Massinen S, Nopola-Hemmi J, Kere J, and Hari R: Human *ROBO1* regulates interaural interaction in auditory pathways. *J Neurosci* 2012, 32: 966–971.

II. **Lamminmäki S** and Hari R: Auditory cortex activation associated with octave illusion. *NeuroReport* 2000, 11: 1469–1472.

III. **Lamminmäki S**, Mandel A, Parkkonen L, and Hari R: Binaural interaction and the octave illusion. *J Acoust Soc Am* 2012, 132: 1747–1753.

IV. **Lamminmäki S**, Parkkonen L, and Hari R: Human neuromagnetic steady-state responses to amplitude-modulated tones, speech, and music. *Submitted.*

The publications are referred to in the text by their roman numerals.

Abbreviations

AEF	auditory evoked field
AEP	auditory evoked potential
ANOVA	analysis of variance
AP	action potential
AVCN	anteroventral cochlear nucleus
BIC	binaural interaction component
BS	binaural suppression
CN	cochlear nucleus
DCN	dorsal cochlear nucleus
DTI	diffusion tensor imaging
ECD	equivalent current dipole
EE	binaural excitatory–excitatory neuron
EEG	electroencephalography
EI (or IE)	binaural excitatory–inhibitory neuron
EOG	electro-oculogram
EPSP	excitatory postsynaptic potential
fMRI	functional magnetic resonance imaging
GABA	gamma-aminobutyric acid
HG	Heschl's gyrus
HL	hearing level
IC	inferior colliculus
ILD	interaural level difference
IPSP	inhibitory postsynaptic potential
ITD	interaural time difference
LE	left ear
LH	left hemisphere
LI	laterality index
LL	lateral lemniscus
LSO	lateral superior olivary nucleus
MEG	magnetoencephalography
MGB	medial geniculate body
MMN	mismatch negativity
MRI	magnetic resonance imaging
mRNA	messenger ribonucleic acid
MTG	middle temporal gyrus
N100m	100-ms response measured by MEG

NLL	nuclei of lateral lemniscus
PAC	primary auditory cortex
PET	positron emission tomography
PSP	postsynaptic potential
PT	planum temporale
PVCN	posteroventral nucleus
qRT-PCR	quantitative real-time polymerase chain reaction
RE	right ear
RH	right hemisphere
ROBO1	human *ROBO1* gene
ROBO1	protein produced by human *ROBO1* gene
ROBO1a	transcript variant 1 of human *ROBO1* gene
ROBO1b	transcript variant 2 of human *ROBO1* gene
SF	sustained field
SLI	specific language impairment
SNR	signal-to-noise ratio
SOC	superior olivary complex
SQUID	superconducting quantum interference device
SSF	steady-state field
SSP	steady-state potential
SSR	steady-state response
STG	superior temporal gyrus
STS	superior temporal sulcus

Abstract

Two functioning ears provide clear advantages over monaural listening. During natural binaural listening, robust brain-level interaction occurs between the slightly different inputs from the left and the right ear. Binaural interaction requires convergence of inputs from the two ears somewhere in the auditory system, and it therefore relies on midline crossing of auditory pathways, a fundamental property of the mammalian central nervous system.

Binaural interaction plays a significant role in sound localization and other auditory functions, e.g. speech comprehension in a noisy environment. However, the neural mechanisms and significance of binaural interaction and the development of crossed auditory pathways are poorly known. This thesis aimed to expand, by means of magnetoencephalography (MEG), knowledge about binaural cortical processing and midline crossing of auditory pathways in subjects with the defective dyslexia susceptibility gene *ROBO1* and in healthy individuals.

Study I demonstrated that in dyslexic individuals who carry a weakly expressing haplotype of the *ROBO1* gene, binaural interaction is strongly impaired as compared with healthy, age- and sex-matched controls. Moreover, the observed impairment correlated with the expression level of the *ROBO1* gene: the weaker the expression, the more abnormal was the binaural interaction. On the basis of previous animal studies and the quite well known anatomy of the subcortical auditory system, we suggest that the normally extensive crossing of auditory pathways is defective in *ROBO1*-deficient dyslexic subjects.

Abstract

All auditory illusions emerging in healthy individuals rely on normal neurophysiology, and thus illusions elicited by binaural sounds can be valuable in revealing auditory binaural processing. Studies II and III examined the neural basis of peculiar pitch perception and sound localization during the auditory octave illusion originally described by Diana Deutsch in 1974. In the octave illusion, dichotic tones separated by an octave alternate rapidly between the ears so that when the left ear receives the low tone, the right ear receives the high tone and vice versa. Study II demonstrated that transient 100-ms responses (N100m), generated in the auditory cortices, follow the sound location perceived during the illusion. Study III further showed that modifications in normal binaural interactions contribute to the illusory pitch perception.

Currently, binaural interaction can be studied non-invasively in detail by means of cortical steady-state responses and MEG-based frequency-tagging. Steady-state responses have also been used in clinical settings to evaluate hearing in non-collaborative patients. Until now, only simple acoustic stimuli have been used to elicit steady-state responses, although in our daily lives we communicate with physically much more complex sounds, such as speech and music. Study IV demonstrated that natural sounds with carefully selected sound parameters can also be used as reliable stimuli in future steady-state studies, and therefore to scrutinize the role and mechanisms of binaural interaction.

This thesis links the dyslexia susceptibility gene, *ROBO1*, to neurodevelopment of auditory system and binaural processing, reveals the sound localization and pitch perception mechanisms during the octave illusion, and provides knowledge about steady-state responses to natural sounds, thereby advancing future binaural interactions studies.

1 Introduction

Two functioning ears provide clear advantages over monaural listening. We are able to locate sound sources in a variety of auditory spaces accurately (≈1 deg) and rapidly, and redirect our attention towards the sound sources. In addition, our speech understanding in noisy and reverberant environments relies largely on interaction between the acoustic inputs of two ears (for a review, see e.g. Schnupp et al., 2011). This binaural interaction occurring during natural binaural listening requires convergence between slightly different inputs from the two ears somewhere in the auditory system and therefore relies on midline crossing of the auditory pathways.

Development of axonal midline crossing is, according to animal studies, regulated by a multitude of attractive and repellent agents and the proteins binding them (for a review, see Tessier-Lavigne and Goodman, 1996). One of the key proteins is regulated in fruit flies by the *robo* gene and in rodent embryos by the *Robo1* gene (Kidd et al., 1998a; Andrews et al., 2006). The human counterpart, *ROBO1* gene, is known as one of the dyslexia susceptibility genes (Nopola-Hemmi et al., 2001; Hannula-Jouppi et al., 2005). In addition, *ROBO1* has been linked to autism (Anitha et al., 2008), and a specific language impairment (SLI) variant has shown linkage to a genetic region around *ROBO1* (Stein et al., 2004). However, the neurodevelopmental functions of the *ROBO1* gene—as well as of all dyslexia candidate genes—are unknown. On the other hand, dyslexia is associated with many different kinds of auditory and other sensory and phonological processing deficits, but their relationship to reading problems remains unsolved.

Binaural hearing improves sound localization and speech comprehension in noisy environments, and problems in binaural processing have been associated with subnormal sound localization and speech understanding, occurring e.g. after cochlear implantation (for a review, see Basura et al., 2009; Johnston et al., 2009; Ramsden et al., 2012). The inability to understand speech in noisy environment is also associated with presbyacusia, the most common form of hearing loss in elderly people, and is often the most distracting and socially displacing symptom. Earlier, the communication problems were explained purely as peripheral defects but more recently, the possible contributing role of defective binaural interaction has been suggested (Frisina and Frisina, 1997; Martin and Jerger, 2005).

The neurodevelopmental disorders linked to the *ROBO1* gene, such as dyslexia and autism, cause significant disability and individual suffering, difficulties in social and working life. Therefore, revealing the neurodevelopmental roles and functions of human *ROBO1* gene is highly important. Although one accurately-functioning ear provides moderate hearing ability, binaural interaction problems leading to speech comprehension difficulties can cause social displacement and depressive symptoms. Altogether, deficits in binaural processing and axonal midline crossing, a prerequisite of binaural interaction, may contribute to large patient groups and remarkable socioeconomic costs.

A great deal of current knowledge of the structure and function of the human auditory central nervous system is based on studies of small mammals and primates. However, human anatomy and physiology differ from animals, and humans use more complicated acoustic signals than animals, e.g. speech and music. Therefore, animal data can never replace human studies. On the other hand, many research methods cannot be used in humans because of their invasive nature. Recent progress in neuroimaging has made it possible to study noninvasively many auditory functions in healthy subjects and various patient groups.

The aim of this thesis is to add to our understanding of cortical binaural processing and crossing of auditory pathways in healthy and *ROBO1*-deficient dyslexic individuals.

2 Review of literature

2.1 Basic anatomy and physiology of the auditory system

The human auditory system, the sensory system sensing our acoustic environment, comprises four anatomically and functionally different parts: outer ear, middle ear, inner ear, and central auditory nervous system, the latter (or only the most distal parts of it) is sometimes called in audiology the retrocochlear part (Fig. 1). The central part comprises auditory brainstem, thalamus and cortex. This thesis focuses on the central auditory part, especially on cortical processing.

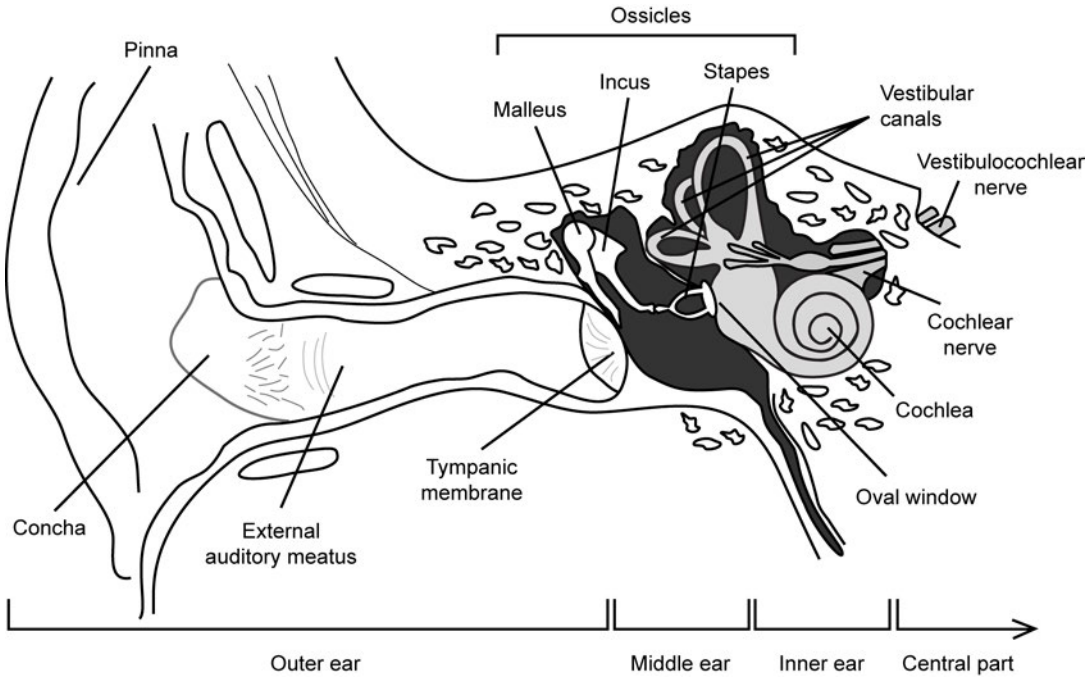


Figure 1. The basic anatomy of the human ear.

The ear converts time-varying air pressure first to mechanical vibration of the bones of the middle ear, then to hydrodynamical movements of the fluids inside the inner ear, and finally to electrochemical signals in neurons and synapses. The auditory cortical structures support the interpretation of the complex neural signals to rich acoustic percepts. The following chapters about the outer, middle, and inner ear are mainly based on the textbooks of auditory anatomy and neuroscience (Yost, 2000; Purves et al., 2004; Schnupp et al., 2011).

2.1.1 The outer and middle ear

The outer and middle ears carry mechanical energy of the sound efficiently from the air outside the head to the perilymph inside the cochlea. Because of the much higher acoustic impedance of the fluid than the air, stronger force is needed to produce corresponding sound waves in the fluid than in the air. If the impedances were not matched, over 99% of the sound energy would be reflected backwards.

The pinna collects the sound and channels it to the external acoustic meatus. At the same time, owing to a complex surface configuration, pinna attenuates some frequencies and causes phase shifts, therefore modifying the perceived sound colour, i.e timbre. The individual changes caused by the head and outer ear to the original sounds, called head-related-transfer-function, help in sound localization, both in the horizontal and the vertical plane. In addition, the resonance of the external acoustic meatus and the concha increases the sound pressure level at 1.5–7 kHz by 10−20 dB.

The tympanic membrane, a thin, 0.1 mm thick 2–3 layer membrane between the outer and middle ear, conveys the mechanical vibration of air to the movements of ossicles (malleus, incus, and stapes). The conical-shape tympanic membrane moves the manubrium of malleus twice as much as the force would otherwise suggest, and the level action of ossicles further force the movements by a factor of 1.3. The middle ear concentrates the sound pressure on the tympanic membrane (a surface area about 0.5 cm^2) to the substantially smaller ($^1/_{30}$–$^1/_{15}$) oval window of the cochlea, resulting in an 800-fold increase in the force of the sound vibrations. The transmission of sound energy via the middle ear is most effective between 500 and 4000 Hz, i.e. frequencies important for speech perception.

2.1.2 The inner ear

The spiral-shaped cochlea translates the mechanical energy into neural responses, i.e. to electrochemical form. When the footplate of the stapes vibrates according to the sound rhythm, the oval window moves inwards and outwards and pressure changes transfer to the perilymph in the scala tympani and distribute immediately to the whole cochlea. Although the inside diameter of the cochlea decreases from the oval window end towards the apex, the basilar membrane broadens and becomes less tensioned, and in consequence, the natural resonant frequencies of the basilar membrane decrease towards the apex. The basilar membrane functions as a band-pass filter with a relatively sharp high-frequency border: low frequencies stimulate primarily the apical but also the basal end, whereas high frequencies stimulate specifically the basal end of the membrane.

The organ of Corti contains the main auditory sensory receptor cells, i.e about 3,500 inner hair cells in each ear, and also over 12,000 outer hair cells that modify the hearing by increasing the sensitivity and frequency resolution of the inner hair cells. The vibrations of the basilar membrane in relation to the tectorial membrane (most probably not directly but via fluid) bend the cilia of the hair cells, and consequently, K^+ ions flow inward to the hair cells from the surrounding endolymph. The depolarized hair cells activate the spiral ganglion neurons, the first real auditory neurons. The spiral cells send long myelinated, rapid (type I) nerve fibers towards the brain stem.

2.1.3 Brain stem and thalamus

The retrocochlear anatomy of the auditory system is very complex, comprising many parallel pathways which cross the midline at multiple levels (see Fig. 2) (for a review, see Kandel et al., 2004; Purves et al., 2004; Kandler et al., 2009; Schnupp et al., 2011). Although the anatomy is fairly well known, the understanding of the auditory functions in the brain stem is still rather poor.

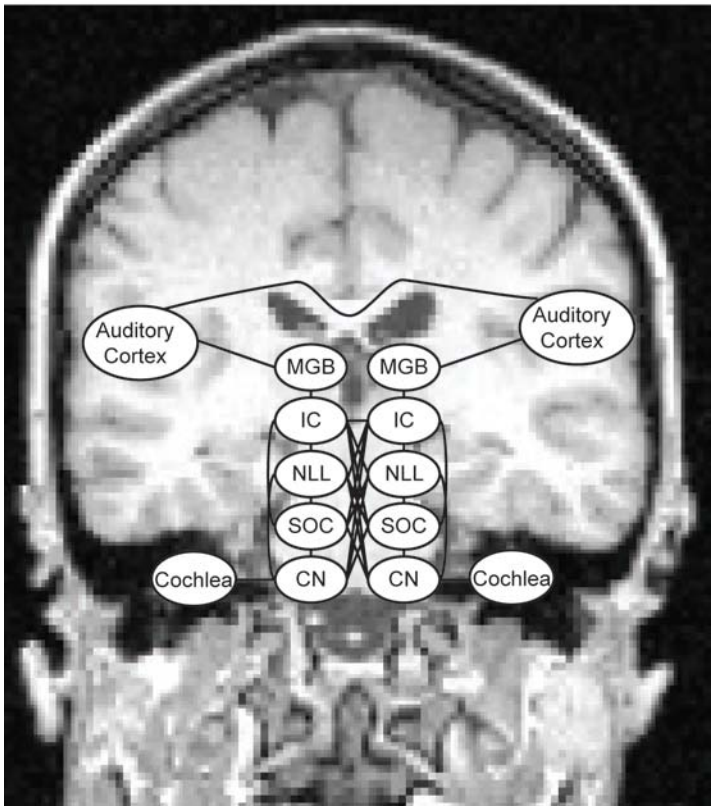


Figure 2. Schematic representation of human auditory pathways on the coronal MRI of a human head. For visual purposes, cochlear nucleus (CN), superior olivary complex (SOC), nucleus of lateral lemniscus (NLL), inferior colliculus (IC), medial geniculate body (MGB), and auditory cortex are shown with ellipses. The black lines indicate neuronal connections between the different parts.

From the cochlea, auditory nerve fibers travel in the vestibulocochlear nerve (the VIII cranial nerve) to the cochlear nucleus, CN, in the lateral part of the brainstem. The CN contains three anatomically and functionally different nuclei: the anteroventral cochlear nucleus (AVCN), the posteroventral nucleus (PVCN) and the dorsal cochlear nucleus (DCN). A single nerve fiber from the cochlea sends inputs to each nucleus: e.g. the bushy cells in the AVCN preserve the accurate temporal firing of the auditory nerve, whereas the stellate cells in the AVCN and the PVCN code the spectral shape of the sound well but remove the timing information, and cells in the DCN respond to spectral contrasts and also receive input from the somatosensory system. The tonotopic organization of the sound is maintained in the whole auditory pathways, although some "nonlemniscal" nuclei remove it.

The different cell types in the CN enter the different parts of the above auditory system: the majority of the axons cross to the opposite side, only about one third projecting to the ipsilateral side. The axons of most cells in the DCN and the stellate cells go directly to the inferior colliculi (ICs) on both sides, whereas bushy cells from the AVCN send axons first to the superior olivary complexes (SOCs). Each SOC receives input from both ipsi- and contralateral ears and plays an important role in sound localization. The neurons from the SOC and the CN travel upwards to the IC in a nerve bundle called lateral lemniscus (LL), some of them sending branches to the nuclei of the lateral lemniscus (NLL). In addition to bilateral input to the IC, left and right ICs are also connected directly, and numerous interneurons inside the ICs are connected in a complicated manner. ICs contain many subnuclei, which are specifically sensitive to temporal regularities in the sound. They send axons primarily to the auditory thalamus, to the medial geniculate body (MGB), but also to the superior colliculus to improve audiovisual integration. Like the IC, the MGB also contains many different subnuclei. Axons from the MGB travel via acoustic radiation to the auditory cortex.

In addition to all ascending pathways, numerous descending auditory pathways travel from auditory cortex to all major nuclei groups in the brain stem and finally from the brain stem back to the cochlea in olivocochlear neuron bundle.

2.1.4 Cortical structures

A great proportion of the human auditory cortex lies deep inside the lateral fissure, in the temporal lobe. Because many research methods are strongly invasive, they cannot be used in healthy humans. Knowledge about the anatomy and physiology of human auditory cortex has been received from post mortem studies, from auditory deficits after different kinds of brain lesions, from direct electric stimulation and recording during epileptic surgery, and from indirect neuroimaging studies. These different research methods, each of them having specific limitations, can provide a complementary view of human brain. However, our understanding about the human auditory system is still largely based on data gathered from small animals and primates. Whereas subcortical auditory structures are rather similar in all mammals, the cortical structures show much more variability between e.g. ferrets, cats, and monkeys, and the borders of areas with possible similar function differ from each other (Hackett et al., 2001; Sweet et al., 2005;

Fullerton and Pandya, 2007; a review by Schnupp et al., 2011). Especially in the second- or higher-order auditory areas, the human auditory anatomy and physiology may differ significantly from the other mammalian counterparts.

In primates, the core of the auditory cortex, consisting of three primary-like areas, is surrounded by a narrow belt area of eight subareas and on the lateral side by the parabelt area (for a review, see Kaas and Hackett, 2000).

2.1.4.1 Primary auditory cortex

In humans, the core auditory area, the primary auditory cortex (PAC), has been separated from the surrounding non-primary auditory areas by using criteria based on cyto-, myelo-, chemo-, and receptor architectonics of the brain (Brodmann, 1909; Galaburda and Sanides, 1980; Rivier and Clarke, 1997; Clarke and Rivier, 1998; Hackett et al., 2001; Morosan et al., 2001; Wallace et al., 2002; Sweet et al., 2005; Fullerton and Pandya, 2007), and by functional data of electrophysiological and fMRI recording (Liegeois-Chauvel et al., 1991; Wessinger et al., 2001; Formisano et al., 2003; Sigalovsky et al., 2006; Da Costa et al., 2011). PAC, corresponding to area 41 in the classic cytoarchitectonic maps of Brodmann (1909) (see Figs. 3A and 3B), is located on the posteromedial two-thirds of the transverse Heschl's gyrus (HG), on the superior plane of the temporal lobe (Hackett et al., 2001; Morosan et al., 2001; Rademacher et al., 2001; Sweet et al., 2005). However, the cytoarchitectonic boundaries of PAC, defined from post mortem brains, do not match perfectly with the macroanatomical landmarks of HG visible in magnetic resonance images (MRI) (Morosan et al., 2001; Rademacher et al., 2001), and the size of the PAC is only 16–92% of the cortical volume of HG (Rademacher et al., 2001). Moreover, the gross morphology of the HG can vary considerably between individuals: single HG is the most common, but partly bifurcated and totally duplicated HG are also rather common (Penhune et al., 1996; Leonard et al., 1998; Morosan et al., 2001; Rademacher et al., 2001). Therefore, relating functional data to microanatomical structures of the auditory cortex is challenging and often impossible.

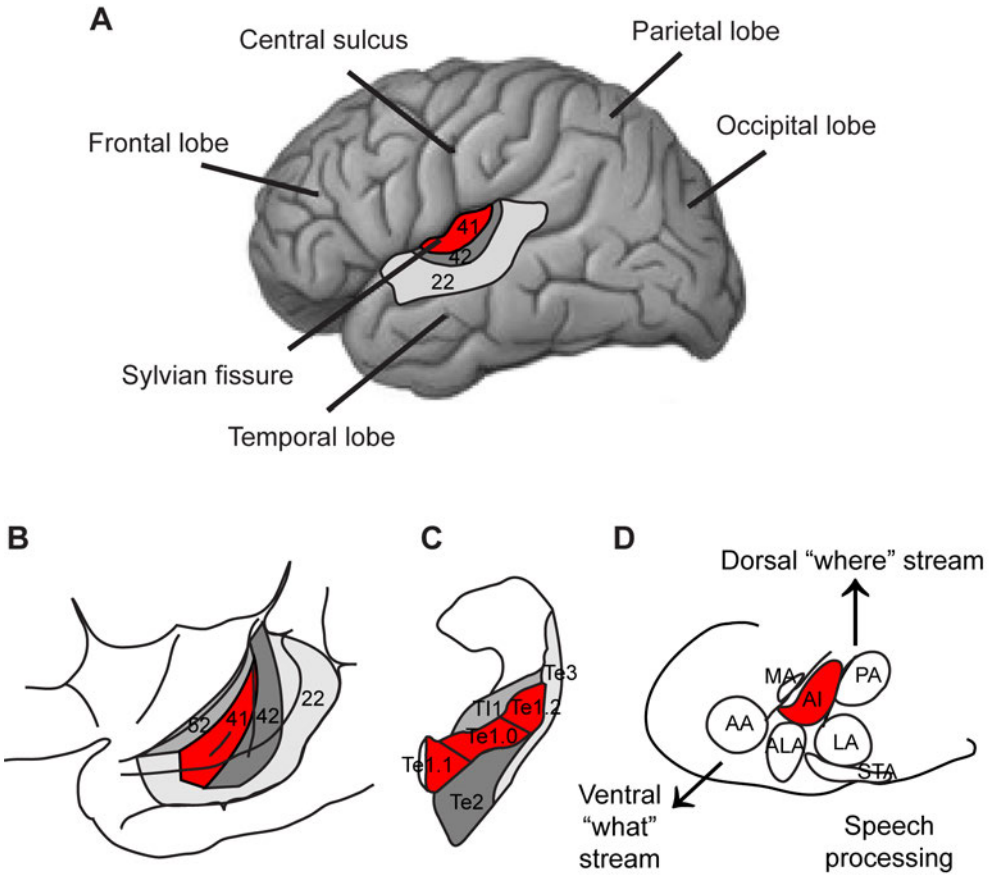


Figure 3. Schematic illustration of human auditory cortex. A) Lateral and B) supratemporal view of the classic cytoarchitectonic maps of the auditory cortex, outlined from (Brodmann, 1909). C) Subareas defined according to observer-independent cytoarchitectonic method (Morosan et al., 2001). D) Primary auditory cortex AI and non-primary auditory areas and their suggested functional roles, outlined from (Rivier and Clarke, 1997; van der Zwaag et al., 2011)

PAC has been further subdivided into two (Galaburda and Sanides, 1980) or three (Morosan et al., 2001) separate areas. According to observer-independent cytoarchitectonic method, PAC contains laterally Te1.2, medially Te1.1, and there between the most highly granular subarea Te1.0 (see Fig 3C). Te1.0 has also the best developed layer IV, probably reflecting strong ascending connection from MGB of thalamus (Morosan et al., 2001).

In the central highly granular core part of the PAC, the cell bodies are arranged into vertical columns (Morosan et al., 2001) and narrow (~500 µm wide) alternating dark and light stripes exist parallel to the long axis of HG (Clarke and Rivier, 1998). The function of the alternating stripes is unknown, but they have been suggested to participate in binaural interaction (Clarke and Rivier, 1998), similarly to vertical columns found in small animals (see the chapter 2.2.1) (for a review about the animal studies, see Imig and Morel, 1983; Ojima, 2011).

PAC contains at least two mirror-symmetric cochleotopic (tonotopic) organizations (Wessinger et al., 2001; Formisano et al., 2003; Talavage et al., 2004; Upadhyay et al., 2007; Humphries et al., 2010; Da Costa et al., 2011; Striem-Amit et al., 2011). Axis of the high-low-high frequency gradient has been suggested to be parallel (Formisano et al., 2003; Upadhyay et al., 2007) or perpendicular to HG (Humphries et al., 2010; Da Costa et al., 2011). In the case of partial/complete duplication of HG, these two subareas with different tonotopy seem to occupy both the anterior and posterior division of HG (Da Costa et al., 2011), contrary to earlier suggestions. According to diffusion tensor imaging (DTI), both the isofrequency areas of the two tonotopic areas and the non-isofrequency areas within each tonotopic area are connected with axonal projections (Upadhyay et al., 2007).

2.1.4.2 Non-primary auditory areas

Similarly to primates, PAC is immediately surrounded by belt and parabelt areas, corresponding mainly to Brodmann's areas 42, 22, and 52 (see Fig. 3A and 3B), and areas Te2, Te3, and TI1 according to Morosan et al. (2001) (see Fig. 3C). Belt and parabelt areas contain several architectonically defined areas (see Fig. 3D): LA, PA, and STA posteriorly in planum temporal (PT), and areas AA, ALA, and MA anteriorly/laterally in planum polare, and in superior temporal gyrus and sulcus (STG and STS) (Rivier and Clarke, 1997; Wallace et al., 2002). Human higher-order auditory areas are involved in processing of complex sounds, such as speech, melody/pitch and auditory objects (see e.g. review by Griffiths, 2001), and the multitude of different areas, compared with primates, probably reflects the complex and elaborate cortical functions in humans (Fullerton and Pandya, 2007). Anterior AA and ALA areas respond bilaterally more to environmental sounds than to localization cues (Viceic et al., 2006), LA and STA are specialized for speech processing (see e.g. review by Scott and

Johnsrude, 2003), and in areas LA, PA, and STA, the spatial information modulates responses to environmental sounds (van der Zwaag et al., 2011). The functional differences found in subareas agree with the separate and parallel "what" and "where" processing streams, found originally in primates (Rauschecker et al., 1997; Kaas and Hackett, 1999; Rauschecker and Tian, 2000; Ahveninen et al., 2006; Recanzone, 2011): areas posterior to PAC participate in spatial "where" processing and the anterior areas in identification ("what" processing) of auditory objects (see Fig. 3D).

Tonotopical organizations with mirror-symmetry have been found also from the non-primary auditory areas, from STG and middle temporal gyrus (MTG), which correspond to the belt and parabelt areas (Striem-Amit et al., 2011).

2.2 Binaural interaction in the auditory system

Two ears provide some clear advantage over unilateral hearing. It has been well known for a long time that sound localization, especially in the horizontal plane, depends critically on the interaction between the inputs of the left and the right ears (for a review, see e.g. Grothe et al., 2010).

Binaural interaction also improves our ability to understand speech in noisy environments (Cherry, 1953; McArdle et al., 2012). Masking of non-relevant sounds in noisy and anechoid environments, e.g. in so called cocktail-party situations with many simultaneous speakers, makes it easier to detect and understand sounds and thus to communicate (Pollack and Pickett, 1958; Cherry and Rubinstein, 2006).

2.2.1 Anatomical basis and physiological mechanisms

Binaural interaction has been revealed mainly in animal brain stems; cortical data especially from humans are still scanty. The brain stem anatomy of the auditory system provides numerous opportunities for different kinds of binaural interactions. In addition, corpus callosum connects the hemispheres via crossing neurons in the splenium.

In the brain stem, binaural interactions occur mainly at three levels: in SOCs, in both NLL and in ICs (for a review, see Moore, 1991). All these nuclei receive both ipsilateral and contralateral projections form the CNs. In addition, between the nuclei travel some minor connections and collaterals, whose role in binaural processing is not well established. Above the level of the tectum, the ascending auditory pathways are purely or predominantly ipsilateral. In addition to ascending pathways, descending pathways may also be involved in binaural processing.

For binaural interaction, an especially important connection exists between the medial nucleus of the trapezoid body and the ipsilateral lateral superior olivary nucleus (LSO): neurons in medial nucleus of the trapezoid body receive excitatory input from the contralateral ear and send inhibitory input to the ipsilateral LSO. Other important connections exist between the central and external nuclei of the IC.

Contrary to many brain stem nuclei, which respond primarily to some binaural features of the input, no clear, anatomically separate areas of different binaural functions have been found in the auditory cortex. Instead, a large proportion, or even all (Zhang et al., 2004), of auditory cortical neurons respond to bilateral stimuli. So called EE (excitatory–excitatory) neurons receive excitatory input from both ears and respond to both monaural (left or right) and binaural stimuli and the binaural stimuli produce stronger responses than monaural. In EI (excitatory–inhibitory) neurons (also called sometimes as IE neurons) inhibition caused by one ear suppresses or even totally dampens the excitation caused by the other ear. EE neurons, but not EI neurons, show strong interhemispheric connections (Imig and Brugge, 1978), whereas IE neurons show stronger connection to specific ipsilateral auditory areas than EE neurons (Imig and Reale, 1981). In humans, no direct evidence about the function of EE and EI cells exist. However, auditory cortical 100-ms responses (N100m) are smaller to binaural stimuli than the sum of monaural responses (Tiihonen et al., 1989). In addition, binaural suppression of steady-state responses is much stronger for ipsi- than contralateral inputs (Fujiki et al., 2002; Kaneko et al., 2003), and the suppression remains similar with a large range in sound loudness (Kaneko et al., 2003).

The best known advantage of binaural interaction—the sound localization ability in the horizontal plane—is mainly based on interaural time differences (ITDs) and interaural level differences (ILDs), as the cochlea does not contain any direct representation of sound location. According to animal studies, all levels of the auditory system from CN to cortex seem to have neurons that respond to specific ITDs and ILDs, e.g. neurons in the medial part of the SOC are sharply sensitive to ITD differences, whereas neurons in the lateral part, LSO, are sensitive to ILD. Although subcortical structures can map sound location cues exactly, they only function as relay stations, and the auditory cortex is necessary for proper sound localization. The cortical mechanisms of localization seem to differ significantly between species and the human mechanisms are still largely unclear (for a review, see Salminen et al., 2012).

2.2.2 Peculiar binaural processing: The octave illusion

Under certain conditions, binaural processing of auditory (typically dichotic) signals can result in inadequate interpretations, i.e. auditory illusions. These perceptual

misinterpretations are based on the normal fundamental auditory mechanisms and can thus be valuable in revealing auditory physiology and binaural processing.

The octave illusion, discovered by Diana Deutch (1974), emerges when dichotic tones that are separated by an octave alternate between the ears so that when the right ear (RE) receives a high tone, the left ear (LE) receives simultaneously a low tone and then *vice versa* (Fig. 4). Most right-handed subjects perceive a monaural sound sequence: a high tone in the RE is alternated with a low tone in the LE (Deutsch, 1974, 1983; Brennan and Stevens, 2002). Thus instead of two simultaneous tones, subjects perceive only a single tone at a time, and during the every other tone pair, the perceived location is in conflict with the perceived pitch. The perceptions of the sounds differ between the left- and right-handed subjects (Craig, 1979; Deutsch, 1983): among the left-handers, the illusory percepts are much more variable.

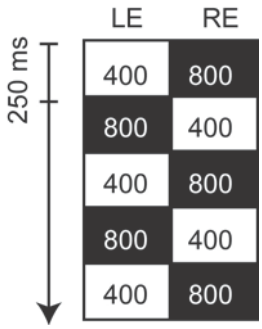


Figure 4. Stimuli eliciting the octave illusion. Adapted from Study III.

The octave illusion is rather resistant to changes in sound parameters: tone duration can alter between 10 ms and 2 s (Zwicker, 1984), an exact octave interval is not necessary (Brancucci et al., 2009), and brief silent gaps in the sound sequence do not distort the illusion (Ross et al., 1996; Chambers et al., 2005).

According to behavioural studies, the perceived pitch follows solely the sound presented to the RE, whereas the perceived location is determined on the basis of the ear receiving the higher-frequency tone (Deutsch, 1974; Deutsch and Roll, 1976; Deutsch, 2004a), but the neural basis of the illusion has not been revealed.

2.3 Human *ROBO1* gene and bilateral neurodevelopment

The human *ROBO1* gene is currently known best as a dyslexia susceptibility gene (Nopola-Hemmi et al., 2001; Nopola-Hemmi et al., 2002; Hannula-Jouppi et al., 2005) but has also been associated with autism (Anitha et al., 2008), and a region around the *ROBO1* gene has shown linkage to an SLI-variant (Stein et al., 2004). In addition, *ROBO1* has been linked to phonological abilities (Bates et al., 2011). However, until now the neurodevelopmental role of *ROBO1* has remained unknown.

The animal counterparts of the human *ROBO1* gene, i.e. *robo* in fruit flies and *Robo1* in rodents, code receptor proteins which in conjunction with the secreted chemorepulsive ligand slit regulate axonal midline crossing and therefore bilateral neuronal connections (Kidd et al., 1998a; Kidd et al., 1998b; Brose et al., 1999; Kidd et al., 1999; Andrews et al., 2006). Mice with homozygous *Robo1* knock-out mutations do not survive after birth, and in mouse embryos, the axons of corpus callosum and hippocampal commissure form large tight fascicles of non-crossing axons at the midline, but in heterozygous knockout mice, all anatomical structures seem normal both in DTI and immunohistochemistry studies (Andrews et al., 2006).

In human and rat embryos (Marillat et al., 2002; Johnson et al., 2009), *ROBO1/Robo1* are expressed around the brain. In the rat fetal auditory system, *Robo1* messenger ribonucleic acid (mRNA) has been seen peripherally in the CNs, in ICs, in medial parts of the dorsal thalamus (nearby the later MGB) and in lateral cortices (Marillat et al., 2002). In humans, *ROBO1* mRNA has been found in temporal-lobe auditory neocortex and in temporal-lobe association neocortex (Johnson et al., 2009). CNs and ICs participate in the formation of bilateral neuronal connections, the prerequisite for binaural interaction, by sending crossing axons to the opposite side (Moore, 1991).

2.3.1 *ROBO1* and developmental dyslexia

Developmental dyslexia (*dys* + Greek *lexis* meaning word), hereafter referred to as dyslexia, is a specific reading disorder (International Classification of Diseases), manifested by difficulty in learning to read despite conventional instruction, adequate intelligence and socio-cultural opportunity (World Federation of Neurology, World

Health Organisation, 1993). Dyslexia, first described in late 1800s as “word-blindness” (Hinshelwood, 1896; Morgan, 1896; Hinshelwood, 1898, 1911), is the most common learning disability, and possibly even the most common neurobehavioral disorder in children (Shaywitz, 1998). The prevalence of dyslexia ranges from about 5 to 10%; in Finland, the prevalence is estimated to be about 6% among adults (Lyytinen et al., 1995).

Already from the beginning of dyslexia research, genetic factors have been suggested to contribute to the development of dyslexia (Morgan, 1896; Hinshelwood, 1911). Until now, several positions in the genome have been linked to dyslexia, and the first six candidate genes have been identified (for a review, see e.g. Kere, 2011; Peterson and Pennington, 2012). However, knowledge about their roles in any human brain function is very sparse.

In a large Finnish family, dyslexia was linked to the pericentromeric region in chromosome 3 (Nopola-Hemmi et al., 2001), and later on to a specific rare haplotype of the *ROBO1* gene in 3p12–q12 (Hannula-Jouppi et al., 2005). In this family, dyslexia seems to be inherited in a dominant manner, co-segregating with the weakly expressing haplotype of the *ROBO1* gene (Nopola-Hemmi et al., 2001; Nopola-Hemmi et al., 2002; Hannula-Jouppi et al., 2005).

During the over 100 years of dyslexia research, a number of different hypotheses and theories of dyslexia have been suggested (see e.g. Habib, 2000). According to a widely supported view, the main problems in dyslexia arise from defective phonological processing (Snowling et al., 2000), i.e. difficulties in breaking up spoken words into simple units (phonemes), mapping letters to the corresponding phonemes, and keeping consecutive phonemes for a moment in the working memory during reading (Rosen, 1999). However, numerous studies have found a multitude of motor and sensory deficits, especially auditory and visual deficits, variably manifested in different dyslexic individuals. These more fundamental low-level processing defects have been suggested to be causally related to phonological problems, or to contribute to some extent to the dyslexia, or to only be epiphenomena of rather minor importance (for a different hypothesis of dyslexia, see: Hari and Renvall, 2001; Stein, 2001; Tallal, 2004; Galaburda et al., 2006; Ahissar, 2007; Goswami, 2011).

2.4 Magnetoencephalography

Magnetoencephalography (MEG) is a non-invasive, safe, and silent electrophysiological method that allows the study of brain activity in both the intact and diseased human brain. Currents in the brain generate weak magnetic fields that can be detected outside the head by an array of extremely sensitive SQUID (Superconducting QUantum Interference Device) sensors inside the MEG system. MEG has an excellent (sub-millisecond) temporal resolution which allows relevant tracking of rapid electrophysiological events in the auditory cortices and other brain areas. By combining MEG data with MRI, the underlying active brain areas can be located with good spatial accuracy (with few mm, Hari, 1990; Hämäläinen, 1991). MEG has been widely used in basic brain research and, increasingly, in clinical diagnostics and follow-up.

This chapter is mainly based on the MEG review articles from our laboratory (Hari and Lounasmaa, 1989; Hari, 1990; Hämäläinen et al., 1993; Hari et al., 2000; Hari, 2004; Hari and Salmelin, 2012) and on neuroscience books (Kandel et al., 2004; Purves et al., 2004).

2.4.1 Physiological basis of MEG signals

The human brain includes approximately 10^{10}–10^{12} neurons connected to each other with even more numerous synapses. Information transmission in the brain is based on cell-to-cell communication, i.e. on several different kinds of electrochemical events in single neurons and in synapses between consecutive neurons.

In the human nervous tissue, all cells are electrically polarized. In ordinary resting state, the inside potential of a neuron is about –70 mV, resulting in a constant voltage across the thin (10 nm) plasma membrane. The potential differences are based on ion concentrations: sodium (Na^+) and chloride (Cl^-) concentrations are much higher outside than inside the plasma membrane, whereas potassium (K^+) concentration is higher inside than outside. The concentration differences are maintained by active ion transporters, i.e. specific proteins embedded into plasma membranes, which carry ions into and out of the neurons against their concentration gradients. The Na^+/K^+ pump, which carries two K^+ ions in and three Na^+ ions out during one cycle, is the most

important for maintaining the plasma membrane gradient. In addition, plasma membranes contain passive, selectively permeable ion channels which allow, when open, specific ions to move in the direction of their concentration gradient. Normally, the membrane is about 100 times more permeable to K^+ than to Na^+, which results, together with the Na^+/K^+ pump function, in a net flux of positive ions out of the cell, thus producing a negatively-charged intracellular medium and the typical resting membrane potential.

In the nervous system, information proceeds mainly by means of rapid electrical impulses (1–2 ms in duration) along axons, i.e. by action potentials (APs). If the inside potential of the neuron rises sufficiently over a critical threshold of about –45 mV, voltage-gated Na^+ channels open in the axon hillock, and an AP initiates. Because of the large electrochemical gradient, Na^+ flows via these open channels rapidly into the neuron, causing depolarization of the neuron. The AP ends with a transient rise in membrane permeability to the potassium and a subsequent outward current of potassium ions which repolarizes the inside potential back to the resting state values, or to an even more negative state (hyperpolarization).

From neuron to neuron(s), signals transmit chemically across the 50-nm-wide synaptic cleft(s). An AP reaching the synapse causes transmitter proteins specific to that neuron to be liberated from their vesicles into the synaptic cleft. These neurotransmitters attach to the neuroreceptors on the plasma membrane of the postsynaptic neuron and allow flow of ions by opening ion-specific channels. These ion flows result in a temporary change in the postsynaptic potential (PSP): depolarization caused by increased positive charge inside the cell makes the neuron fire an AP more easily and is thus called an excitatory postsynaptic potential (EPSP), whereas increased negative charge inside the cell cause hyperpolarization, i.e. an inhibitory postsynaptic potential (IPSP). In the human nervous system, the main excitatory neurotransmitter is the amino acid glutamate, whereas gamma-aminobutyric acid, GABA, is the main inhibitory neurotransmitter.

All changing electric currents produce varying magnetic fields around them. However, in an ideal spherical volume conductor, radial primary currents do not produce magnetic fields outside the sphere. Because the human head is roughly spherical, the MEG

signals detected outside the head are mainly produced by tangential currents. However, two thirds of the human brain surface and all main sensory areas are situated in the fissures, therefore pyramidal neurons in the fissural cortex are tangential to the head surface. Moreover, only a minority of the currents in the human brain is completely radial, meaning that the majority produce a tangential component accessible to MEG.

Large pyramidal cells form one important group of cortical neurons. The weak magnetic fields measurable outside the head by MEG likely derive from synchronous PSPs in the apical dendrites of thousands (10^5 or more) of simultaneously active parallel pyramidal cells (Hari et al., 1980; Hari, 1990; Hämäläinen et al., 1993; Okada et al., 1997; Murakami and Okada, 2006). Unlike rapid APs, PSPs last tens of milliseconds and thus allow effective temporal summation. Secondly, APs can be approximated with a current quadrupole and PSPs with a current dipole. Consequently, magnetic fields produced by APs of cortical neurons can be detected only at very close distances, whereas fields produced by PSPs decrease more slowly as a function of distance.

2.4.2 MEG in the study of auditory processing

The development of MEG started about four decades ago when the brain's magnetic fields were measured for the first time with an induction coil magnetometer (Cohen, 1968). A few years later, utilization of recently developed SQUID sensors improved the method significantly (Cohen, 1972).

Human auditory cortical mechanisms can be studied conveniently with MEG, because human auditory cortices are located in the Sylvian fissures where the main current flow is tangential in respect to the skull. Moreover, auditory stimuli are well suited for MEG because sounds can be generated outside the measurement room and easily conveyed to the subject via e.g. plastic tubes without producing any significant magnetic interference. Accordingly, MEG has been used to study auditory cortical processing since the early days: the magnetic responses evoked by auditory stimuli were first published in 1978 (Reite et al., 1978) and their generators were first unravelled by Hari et al. (1980).

In the early 1980s, distributions and sources of the 100-ms auditory evoked fields were determined (Elberling et al., 1980; Hari et al., 1980), and the tonotopic organization in the auditory cortex was revealed (Romani et al., 1982). MEG was used to study different aspects of auditory processing extensively, e.g. the effects of interstimulus interval (Hari et al., 1982), pitch changes (Hari et al., 1984), and attention (Hari et al., 1989b). Studies of cochlear implant users (Hari et al., 1988; Pelizzone et al., 1991) revealed different cortical processing of inputs to congenitally deaf than from the acquired-to-deaf ear (the early results are reviewed e.g. in Hari, 1990; Mäkelä and Hari, 1990; Sams and Hari, 1991; Hari and Salmelin, 2012).

In 1992, the world's first whole-scalp neuromagnetometer was introduced in Finland, in the Low Temperature Laboratory at the Helsinki University of Technology (Kajola et al., 1991; Ahonen et al., 1993). The whole-scalp coverage with 122 gradiometer channels provided excellent spatio-temporal resolution and allowed reliable co-registration of the functional MEG data with anatomical MRIs. This device allowed, for the first time, activity of both hemispheres to be measured simultaneously, and the differences in hemispheric activity (i.e. ipsi- and contralateral activity for monaural stimuli) became easy to see directly from the measured raw data without any extra processing (Mäkelä et al., 1993; Pantev et al., 1998).

With MEG, pathological auditory cortical processing has been successfully revealed in many diseases, e.g. studies done in our laboratory have examined unilateral hearing loss (Vasama et al., 1994; Vasama et al., 1995), ischemic lesions and stroke (Mäkelä et al., 1991; Mäkelä and Hari, 1992), and auditory hallucinations (Tiihonen et al., 1992). In dyslexic individuals, many different kinds of changes in auditory processing have been found (Hari and Kiesilä, 1996; Hari et al., 1999; Helenius et al., 1999; Helenius et al., 2002; Renvall and Hari, 2002, 2003; Parviainen et al., 2005).

Recently, two MEG devices separated by 5 km in the Helsinki-Espoo region have been connected to allow studies of real-time auditory interaction between two persons to aim for "2-person neuroscience" (Baess et al., 2012). Combining of simultaneously measured MEG-data of two persons may provide information of brain-to-brain interactions and inter-subject coupling during natural real-time social interaction.

2.4.2.1 Auditory evoked responses in MEG

Auditory evoked fields (AEFs) measured by MEG, as well as the corresponding auditory evoked potentials (AEPs) measured by electroencephalography (EEG), are typically classified according to their latencies from the sound onset. Typical AEFs to sound stimuli have several different deflections with slightly different field patterns, indicating changing cortical activation as a function of time, and separate, not necessarily sequential, underlying neural processes.

The earliest cortical auditory response detected with MEG peaks at about 11 ms after the sound onset (Kuriki et al., 1995). Several so-called middle-latency responses have been found and categorized by means of EEG (Na at 19 ms, Pa at about 30 ms, Nb at 40 ms and Pb (aka P1) at about 50 ms, N indicating scalp-negativity and P scalp-positivity in a conventional EEG setup). In MEG studies, Pam, the neuromagnetic counterpart of the 30-ms deflection, is detected reliably and consistently, whereas the other middle-latency responses have been found more variably (Pelizzone et al., 1987; Scherg et al., 1989; Mäkelä et al., 1994; Godey et al., 2001). According to both MEG (Pelizzone et al., 1987; Hari, 1990; Godey et al., 2001) and intracranial recordings (Godey et al., 2001), the neuronal origin of the 30-ms response is in the Heschl's gyrus.

The most prominent magnetoencephalographic response, N100m, peaks about 100 ms after the sound onset (Hari et al., 1980; for a review, see Hari, 1990) and is elicited by any abrupt sound or change in sound. The neuronal sources of N100m were first identified by Hari et al. (1980) to be in the supratemporal auditory cortex. N100m is generated in the lateral HG and in the PT, i.e. lateral and posterior to the PAC (Godey et al., 2001; Ahveninen et al., 2006). N100m is typically slightly larger (Elberling et al., 1982; Pantev et al., 1986; Hari and Mäkelä, 1988; Mäkelä et al., 1993) and 4–9 ms earlier (Elberling et al., 1981; Hari and Mäkelä, 1988; Mäkelä et al., 1993) to contralateral than to ipsilateral sounds. The strength of N100m responses increases with increasing sound volume, reaching a plateau at about 60 dB hearing level (HL) (Elberling et al., 1981; Reite et al., 1982; Bak et al., 1985). For binaural stimuli, N100m responses can be equal (Reite et al., 1982) or weaker (Pantev et al., 1986; Tiihonen et al., 1989) than the contralateral responses, indicating suppressive binaural interaction (Pantev et al., 1986). Although N100m can be elicited by many different kind of

sounds, many stimulus parameters contribute to it (Pantev et al., 1988), suggesting that it carries stimulus-specific information, e.g. about sound location (Tiihonen et al., 1989; McEvoy et al., 1994).

N100m is typically followed by an opposite deflection, P200m, and for long (over 400 ms tones) by sustained fields (SFs) lasting a bit after the sound offset (Hari et al., 1980; Hari et al., 1987; for a review, see Hari, 1990). SFs originate in the STG, anterior to sources of N100m (Hari et al., 1987; Mäkelä and Hari, 1987), close to the lateral side of PAC (Keceli et al., 2012), and is sensitive to periodicity of sound stimuli (Gutschalk and Uppenkamp, 2011; Keceli et al., 2012).

2.4.2.2 Steady-state responses to long periodic sounds

Various long, periodically repeated sounds, such as amplitude- or frequency-modulated tones or trains of regularly repeated tone bursts, can elicit sinusoidal steady-state responses (SSRs) (for a review, see Picton et al., 2003). Click-evoked steady-state potentials (SSPs) measured by EEG were first reported in 1981 by Galambos et al., and the corresponding click-evoked steady-state fields (SSFs) were recorded by MEG six years later (Mäkelä and Hari, 1987).

SSRs are generated in the PAC and the surrounding supratemporal regions (Mäkelä and Hari, 1987; Hari et al., 1989a; Gutschalk et al., 1999). They are the strongest at around 40 Hz repetition rate (Galambos et al., 1981; Stapells et al., 1984; Hari et al., 1989a), suggested to result from superimposition of consecutive middle-latency responses (Galambos et al., 1981; Hari et al., 1989a). The amplitude of the 40-Hz SSRs decreases when the carrier frequency increases (Stapells et al., 1984; Kuwada et al., 1986; Rodriguez et al., 1986; Pantev et al., 1996; Ross et al., 2000). To continuous modulated tones, the strength of the SSRs decreases with the decreasing modulation depth (Kuwada et al., 1986; Rees et al., 1986; Ross et al., 2000; Picton et al., 2003).

SSRs also decrease with the decreasing stimulus intensity and disappear near the hearing threshold—this feature of SSPs has been applied in clinical practice as an objective way to test hearing thresholds in non-collaborative subjects (John et al., 2004; Canale et al., 2006; Lin et al., 2009; Rosner et al., 2011; Brennan et al., 2012).

2.4.2.3 MEG-based frequency-tagging to study binaural interaction

Until recently, binaural interaction has been studied mostly with behavioural tests as well as with binaural interaction component (BIC) metrics (Delb et al., 2003) of electrophysiological recordings. BIC, introduced in 1979 (Dobie and Berlin), is the arithmetical difference between the sum of monaurally-evoked responses and responses caused by binaural stimulation by the same sounds. BIC demonstrates the decrease (inhibition) of responses during binaural stimulation and has been applied to both noninvasive and invasive electrical recordings. However, BIC is unable to quantify inhibition of the responses to the left and right ear inputs separately.

Normally, the auditory input from one ear reaches the auditory cortices of both hemispheres; thus, during binaural hearing, each hemisphere responds to both left- and right-ear inputs. Unlike with BIC, these response components can be separated from each other by the MEG-based frequency tagging method developed in our laboratory: the LE- and the RE-stimuli are amplitude-modulated with slightly different frequencies, and the resulting SSRs are separated from each other by means of the modulation frequencies (Fujiki et al., 2002). Therefore, frequency tagging enables ipsi- and contralateral responses to be studied separately and binaural interaction quantified in much more detail than with other methods. Typically, responses to one ear input, presented to the same ear, are significantly weaker during binaural than monaural presentation, and this binaural suppression (BS) is in healthy subjects stronger for ipsilateral than for contralateral responses (Fujiki et al., 2002; Kaneko et al., 2003). In addition to cortical processing, subcortical binaural processing can be studied indirectly by means of frequency tagging.

2.4.2.4 Benefits and drawbacks of MEG in auditory studies compared with EEG

MEG and the much more commonly used EEG are closely related electrophysiological methods. Although MEG measures magnetic fields and EEG electric potentials, the underlying primary currents in the brain are the same. Currently, MEG and EEG are the only non-invasive brain imaging methods with a sub-millisecond-scale temporal resolution. These two methods have many similarities but also important differences.

MEG has some clear benefits over EEG in studying (auditory) cortical processing. Unlike EEG signals, tissues outside the brain (e.g. skull, scalp and meninges) do not distort and smear MEG signals (for a review, see Hari, 2004), and thus the spatial resolution of MEG is much better; in auditory cortex, 5 mm relative spatial resolution can be easily achieved (Hari and Mäkelä, 1988), and in favourable conditions even 2–3 mm. EEG signals receive contributions from both radial and tangential currents whereas MEG is rather selective to tangential currents in the fissural cortex, such as the auditory cortices located in the wall of the Sylvian fissure. In addition, MEG is reference-free, whereas the EEG signals depend on the selected reference electrode. As a result, analysis of MEG signals is more straightforward, and e.g. in auditory studies, responses from the two hemispheres are clearly separable.

For both methods, the spatial accuracy is best for superficial sources. In an ideal head, the spatial accuracy of MEG is 1/3 better than that of EEG (Cuffin and Cohen, 1979; Cohen and Cuffin, 1983; for a review, see Hari, 2004). However, in real situations, conductivities of all tissues in the head are not known and cannot be taken into account, and thus the spatial accuracy of MEG is clearly better than that of EEG (Anogianakis et al., 1992).

MEG instrumentation is much more expensive and requires a non-noisy environment, whereas EEG is portable and well suited both to the bedside monitoring of patients and recordings during movements (e.g. epilepsy seizures). In MEG, no measurement electrodes and thus no problems in skin connection exist and the preparation time is therefore shorter.

MEG and EEG can provide complementary information about brain function (see e.g. Gutschalk et al., 2010), and together they produce better source localization than MEG alone (Fuchs et al., 1998).

2.4.2.5 MEG vs. PET, fMRI and intracortical recordings

Compared with MEG, positron emission tomography (PET) and functional magnetic resonance imaging (fMRI) have better spatial resolution, whereas their temporal resolution is much poorer. In auditory research, the total silence of MEG is a clear advantage over the very noisy fMRI.

MEG results can be combined effectively with fMRI/PET data: active brain areas are first determined with PET or fMRI, and then this knowledge is used in source modelling of MEG data. However, in similar experimental setups, MEG and fMRI data can also differ clearly (Furey et al., 2006; Liljeström et al., 2009; Nangini et al., 2009; Gutschalk et al., 2010; Vartiainen et al., 2011) and MEG can detect signals/brain functions that do not produce any changes in PET/fMRI (e.g. very rapid events).

Intracranial recordings and stimulation can provide valuable knowledge about auditory processing and the active brain areas straight from the cortex, but their usability for humans is limited. On the other hand, intracranial recordings in animals can never replace knowledge received from humans.

3 Aims of the study

The aim of this thesis was to investigate auditory cortical processing, in particular binaural interaction in healthy subjects and in individuals with a defective dyslexia susceptibility gene, *ROBO1*. The specific aims of the studies were the following:

(i) To examine binaural interaction and crossing of auditory pathways in individuals who carry the weakly expressing haplotype of a dyslexia susceptibility gene, *ROBO1* (Study I).

(ii) To investigate the neural correlates of sound localization and pitch perception of defective percepts during the octave illusion (Study II).

(iii) To find out how binaural interaction contributes to pitch perception during the octave illusion (Study III).

(iv) To find out the usability of steady-state responses evoked by naturalistic sounds—amplitude-modulated speech and music—in further studies of binaural interaction and other early auditory cortical processing (Study IV).

4 Materials and methods

4.1 Subjects

Altogether 10 dyslexic individuals with a specific *ROBO1* gene defect and 45 healthy volunteers participated in the MEG studies. Six out of the 45 healthy subjects participated in two or three different studies. In Study III, the data of four subjects were rejected because of too poor signal-to-noise ratio or technical problems. In the genetic part of Study I, blood samples of 10 anonymous healthy blood donors were used as control data.

All subjects of the MEG studies were right-handed according to the Edinburgh Handedness Inventory. The studies were approved by a local ethics committee and an informed consent was signed by each subject.

	N	F, M	MEAN AGE	AGE RANGE
Study I *ROBO1*	10	4, 6	31.0	19–51
Study I healthy	10	4, 6	31.8	18–49
Study II	12	8, 4	25.0	22–36
Study III	15	9, 6	29.1	19–47
Study IV	11	4, 7	25.8	20–39

Table 1. Subjects of the MEG studies. F refers to females, M to males; age is given in years.

4.1.1 *ROBO1*–deficient dyslexic subjects

The *ROBO1*-deficient dyslexic subjects of Study I belong to the same Finnish family and carry a partial haploinsufficiency of the *ROBO1* gene, meaning that they have one normal copy and one weakly expressing copy of the gene (Hannula-Jouppi et al., 2005). In the family, this specific weakly-expressing haplotype of the *ROBO1* gene co-segregates with dyslexia in a dominant fashion, and both the haplotype and diagnosed dyslexia have been found in 19 family members (Nopola-Hemmi et al., 2001; Nopola-Hemmi et al., 2002).

The dyslexia diagnosis of each subject was verified during the earlier study by careful neuropsychological tests: two of our subjects have severe dyslexia, five subjects mild or compensated dyslexia, and the remainding three subjects were not categorized according to the severity of their dyslexia since they were under 13 years of age at the time of testing (Nopola-Hemmi et al., 2002).

4.1.2 Hearing levels

In Studies II–IV, all subjects had normal hearing. In Study I, three subjects with *ROBO1* gene defect had noise-induced hearing loss (max 40 dB HL) between 4000 and 6000 Hz; between 125 and 3000 Hz their audiograms were normal (< 20 dB HL, tested in a silent, non-soundproof room).

Before the MEG measurement, the hearing thresholds were further tested with the applied stimuli (e.g. pure tones, amplitude-modulated tones/music/speech), separately for each ear. No significant hearing loss or differences between the ears were observed.

4.1.3 Psychophysical tests

In Study II, 11 out of the 12 subjects of the MEG measurement also participated in the additional psychophysical test. For Study III, 42 right-handed subjects were screened via behavioural testing, and 19 of them were selected according to their percepts to the MEG measurement.

4.2 MEG recordings

4.2.1 Stimulation

In all studies of this thesis, auditory stimuli were delivered to the subjects' ears through plastic tubes and ear pieces. Before the measurement, the sound intensities were adjusted to the highest comfortable listening level, and then balanced between the ears.

In Study II, the stimuli were 500-ms tones, presented either dichotically (i.e. different frequency in the LE and the RE) or binaurally with the same tone in both ears. In Studies I, III and IV, 90–120-s amplitude modulated tones were presented both binaurally and monaurally. In addition to tones, Study IV also included amplitude-modulated 90-s long natural sounds, speech and music.

4.2.2 Recordings

The MEG recordings were carried out in the magnetically-shielded room in the Brain Research Unit of the O.V. Lounasmaa Laboratory at Aalto University (previously Brain Research Unit, Low Temperature Laboratory, Helsinki University of Technology); the shielding made of μ-metal and aluminium protects against the fluctuations in the magnetic field of the earth, power lines, moving vehicles, radio transmitters, etc. The brain's magnetic fields were measured by sensitive SQUID sensors because typical MEG signals are extremely weak (about 10^{-15} T), only 10^{-8} times the steady magnetic field of the earth.

Cortical responses to auditory stimuli were measured with whole-scalp neuromagnetometers: in Study II with a 122-channel Neuromag-122™ device (Ahonen et al., 1993; Knuutila et al., 1993), and in Studies I, III, and IV with a 306-channel Vectorview™ device (Neuromag Oy, Helsinki, Finland; currently Elekta). The Neuromag-122™ system contains 122 planar first-order gradiometers (i.e. figure-of-eight shaped coils) arranged into dual units at 61 measurement sites. In the Vectorview system, the 306 sensors are arranged in 102 units, each housing one magnetometer and two planar first-order gradiometers. The analyses of all studies were based on the signals of planar gradiometers, which measure the two orthogonal gradients (x and y) of

the magnetic field approximately normal to the skull and show maximum signal directly above an active brain area (i.e. where the magnetic field gradient is strongest).

Structural MRIs of Study II were obtained at the Department of Radiology, Helsinki University Central Hospital, with a 1.5T Magnetom™ scanner (Siemens GmbH, Erlangen, Germany). For Studies I, III, and IV, MRIs were obtained at the Advanced Magnetic Imaging Centre, Aalto University, with a 3.0T Signa™ Excite scanner (General Electric, Inc., Milwaukee, WI, USA).

For co-registering the functional MEG data with anatomical MRIs, the position of the head with respect to the MEG sensors was quantified before the MEG recordings. Four head position indicator coils were attached to the subject's head (behind the earlobes and on the both sides of forehead) and their positions with respect to the individual anatomical landmarks (preauricular points and nasion) were determined with a 3D-digitizer. The position of the subject's head inside the sensor helmet was quantified by sending small currents to the indicator coils and by measuring the resulting magnetic fields with MEG sensors.

During the experiments, the subjects were sitting with the head leaning against the sensor helmet and were instructed to keep their eyes open. The measurements session lasted 30–60 min.

The MEG signals were bandpass filtered at 0.03–200 Hz in Studies I and III, at 0.03–130 Hz in Study II, and at 0.1–200 Hz in Study IV. The sampling frequency was 600 Hz except in Study II where the signals were sampled at 390 Hz.

Because eye movements and blinks produce artefacts to the measured MEG signals (Antervo et al., 1985), the MEG data of Studies I, II, and IV coinciding with >150 μV electro-oculograms (EOGs) were rejected from further analysis. In Study III, no EOG-based rejection was used because the analysis focused on frequencies between 32–48 Hz and artifacts related to eye blinks and eye movements occur at much lower frequencies (under 1 Hz). In addition to EOG rejection, MEG signals with large fluctuations (over 3000 fT/cm in gradiometer channels) were considered contaminated and thus rejected from further analysis.

4.2.3 Data analysis

In all studies, signal-to-noise ratio (SNR) was improved by signal averaging (i.e. by suppressing random, stimulus-independent noise). In Study II, the analysis period for the transient responses was 1100 ms, including 150-ms prestimulus baseline, and for each stimulus category, about 100 responses to the repeated stimuli were averaged. In Studies I, III, and IV—all focusing on the weak SSFs produced by long amplitude-modulated sounds—about 2000 time epochs, each comprising six cycles of the applied modulation frequency (corresponding to 146–153 ms), were averaged time-locked to the modulation.

The magnetic fields measured by the planar gradiometers were modelled with point-like equivalent current dipoles (ECDs). For source modelling, the head was assumed to be a spherically symmetric volume conductor with dimensions derived from the individual MRIs when available. This head model was considered adequate since in the temporal lobes, where the auditory areas are located, the accurate realistic-shaped head model would not provide significant benefits (Hämäläinen and Sarvas, 1989; Hari, 1990; Tarkiainen et al., 2003). Two ECDs that best explained the field variability in 26–28 gradiometer channels over each temporal lobe (goodness-of-fit > 80%) were found by least-square fits, and when possible, the locations of the ECDs were verified on the subject's own MRIs.

In Studies I and III, ECDs fitted to monaural responses were also used to model the responses elicited by corresponding sounds during binaural stimuli. Similarly, in Study IV, ECDs derived from responses to the most strongly amplitude-modulated tones were also used to model responses to other applied stimuli.

In addition to source analysis, Studies I and II applied channel-level data-based analysis. Vector sums were calculated from the responses measured by the two orthogonal gradiometers (the squared values of two signals were summed, and then the square root of the sum was computed, separately for each time point). In Study I, vector sums of four adjacent gradiometer pairs including the maximum response in that temporal lobe were averaged.

In Studies I, III and IV, which examined the sinusoidal steady-state responses, the strengths of the responses were measured as peak-to-peak values, and in Study II as deflections from the baseline.

Hemispheric laterality of the source strengths was quantified in Studies II and III with laterality index (LI): LI = (R – L) / (R + L), where R denotes the response strengths in the right hemisphere (RH) and L respectively in the left hemisphere (LH). LI value –1 indicates pure LH activity whereas pure RH activation results in LI value +1.

In Studies I and III, the typical decrease of SSF strength during binaural stimulation, as compared with responses evoked by monaural listening of the same sound in the same ear (Fujiki et al., 2002; Kaneko et al., 2003), was quantified with binaural suppression (BS): BS = (1 – BIN / MON) * 100%, where BIN and MON refer to source strengths during binaural and monaural stimulation. A positive BS value means that SSFs to a binaural stimulus are weaker than SSFs to the corresponding monaural stimulus (same sound presented to the same ear), whereas a negative BS value indicates the reversed condition.

The statistical significances were assessed with paired, two-tailed t-tests and different forms of analysis of variance (ANOVA). Pearson's correlation coefficients were calculated to quantify correlations.

4.3 Genetic tests

The *ROBO1*-deficient dyslexic subjects of Study I had participated earlier in genetic studies (Nopola-Hemmi et al., 2001; Nopola-Hemmi et al., 2002; Hannula-Jouppi et al., 2005), showing that they carry the same rare, weakly-expressing haplotype of *ROBO1* gene. For measuring the individual total expression levels of the *ROBO1* gene, messenger ribonucleic acid (mRNA) levels were determined with quantitative real-time polymerase chain reaction (qRT-PCR). In addition, expression levels of the two different transcript variants, *ROBO1a* and *ROBO1b*, were determined similarly by using the comparative threshold cycle method. For dose analysis with MEG data, the qRT-PCR-data were first normalized to the geometric mean of two reference genes, *GAPDH* and *18SrRNA*, and then to the highest measured individual value.

5 Experiments

5.1 Binaural interaction is abnormal in individuals with a *ROBO1* gene defect (Study I)

In the human central nervous system, auditory pathways as well as brain commissures and a majority of the all afferent and efferent pathways cross the midline before reaching the cerebral cortex. According to animal studies, the midline crossing is regulated by the *robo* and *Robo1* genes, the animal counterparts of the human *ROBO1* (Kidd et al., 1998a; Kidd et al., 1998b; Andrews et al., 2006). The human the *ROBO1* is known best as a dyslexia susceptibility gene (Fisher et al., 2002; Hannula-Jouppi et al., 2005), but the neurodevelopmental role of the *ROBO1* gene remains unclear.

In this study, we aimed to reveal the unknown function and significance of *ROBO1* gene in human development by studying auditory processing and crossing in auditory pathways in 10 dyslexic subjects with the same rare, weakly expressing *ROBO1* gene, and in healthy control subjects.

Because animal studies indicate that only total *robo/Robo1* gene defects generate clear—and lethal—anatomical abnormalities in neural pathways, whereas structures of individuals with a partial defect seem normal (Andrews et al., 2006), we studied crossing in auditory pathways with a sensitive functional approach to quantify binaural auditory interactions. So far no individuals with a totally inactive *ROBO1* gene have been found.

Normally, cortical SSFs to a certain sound presented to one ear are weaker during binaural than monaural stimulation. This binaural suppression relies on the convergence of the LE and the RE inputs, and therefore on the crossing in auditory pathways. Because suppression has to rely on crossing of contralateral pathways for ipsilateral (non-crossing) inputs, we hypothetized that ipsilateral suppression is decreased in subjects with *ROBO1* gene defects. Ipsilateral suppression is also typically clearly stronger than contralateral suppression.

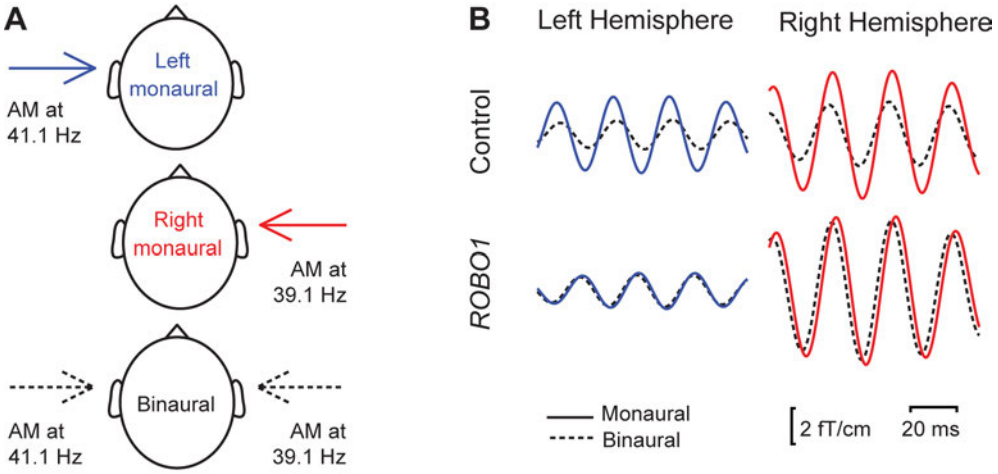


Figure 5. A) Stimuli used in the frequency-tagging. Left-ear inputs are amplitude modulated (AM) at 41.1 Hz and right-ear inputs at 39.1 Hz. B) Steady-state responses to ipsilateral stimuli. Modified from Study I.

5.1.1 Results

In all dyslexic subjects with the *ROBO1* gene defect and in all healthy control subjects, the monaurally and binaurally presented amplitude-modulated tones (1 kHz carrier frequency modulated at 41.1 Hz for the LE and at 39.1 Hz for the RE, see Fig. 5A) elicited clear sinusoidal SSRs in both temporal lobes. In control subjects, the binaural responses were clearly suppressed as compared with corresponding monaural responses, and this suppression was stronger for ipsilateral than contralateral inputs ($F(1,9) = 27.67$, $p < 0.001$, see single-channel responses for ipsilateral inputs in Fig. 5B). In *ROBO1*–deficient dyslexic subjects, the ipsilateral suppression was statistically significantly weaker than in the control group ($F(1,18) = 7.78$, $p < 0.012$), and in both hemispheres, the suppression became more abnormal along with the weakening *ROBO1* gene expression level (Pearson's correlations in the LH, $r = 0.75$, $p < 0.02$ and in the

RH, $r = 0.78$, $p < 0.01$). In contralateral suppressions, no statistical difference between the groups was found.

In both groups, the expression levels of a shorter transcript variant, *ROBO1b*, correlated very strongly with the total *ROBO1* expression levels ($r > 0.99$), whereas the longer transcript variant, *ROBO1a*, was not expressed in lymphocytes at a detectable level.

5.1.2 Discussion

In line with our hypothesis, binaural auditory interaction, as measured at the cortical level, was abnormal in subjects with a weakly expressing haplotype of the *ROBO1* gene. Specifically, ipsilateral suppressions were clearly weakened, and the impaired suppressions depended on the *ROBO1* expressions in a dose-dependent manner. According to animal studies (Kidd et al., 1998a; Kidd et al., 1998b; Andrews et al., 2006) and the well established anatomy of the human auditory system (Moore, 1991; Purves et al., 2004), we suggest that the impaired ipsilateral suppression results from the abnormal crossing of auditory pathways.

The results of expression analysis indicate that in our dyslexic subjects at least the expression of *ROBO1b* is abnormally weak. In the auditory cortices of human embryos, expression of *ROBO1a* is stronger than expression of *ROBO1b*, and the *ROBO1a* expression concentrates especially on the auditory cortices (Johnson et al., 2009). However, we were not able to evaluate *ROBO1a* expression since it was not detected in lymphocytes at a reliable level—in line with earlier animal studies (Clark et al., 2002; Nural et al., 2007).

Our study demonstrates, for the first time, the significance of an adequate *ROBO1* expression level for normal auditory processing, and links a specific sensory function to a dyslexia susceptibility gene. The results agree with the animal data about the role of *ROBO1* orthologs in neurodevelopment (Kidd et al., 1998a; Kidd et al., 1998b; Brose et al., 1999; Kidd et al., 1999; Andrews et al., 2006).

5.2 Auditory transient responses to dichotic tones follow the sound localization during the octave illusion (Study II)

In the auditory octave illusion (Deutsch, 1974) elicited by alternating dichotic tone pairs (see Fig. 4), most right-handed people perceive a sound sequence of monaural tones that alternate between the ears: the high tones are perceived in the RE and the low tones in the LE. Thus, the perceived pitches are imperfect, and the perceived sound locations disagree with every second perceived pitch (Deutsch, 1974; Deutsch and Roll, 1976; Deutsch, 2004b). Dichotic tones have been widely used to study binaural interaction and we aimed to investigate the neural basis of impaired pitch perception and sound location emerging during the octave illusion.

5.2.1 Results

In both hemispheres, both dichotic pairs of the 400 and the 800 Hz tones elicited stronger N100m responses than the tone pairs where both ears received the same tone ($p < 0.0008$). Figure 6 demonstrates that the order of the strengths of transient N100m responses to the dichotic pairs tended to be opposite to the order of the strengths of the longer-lasting SFs. In both hemispheres, the difference between the normalized N100m responses and the SFs was stronger for the dichotic tone pair, where the contralateral ear received the higher (800-Hz) tone, and they corresponded to the perceived location in the illusion (in the LH $p < 0.003$, in the RH $p < 0.002$).

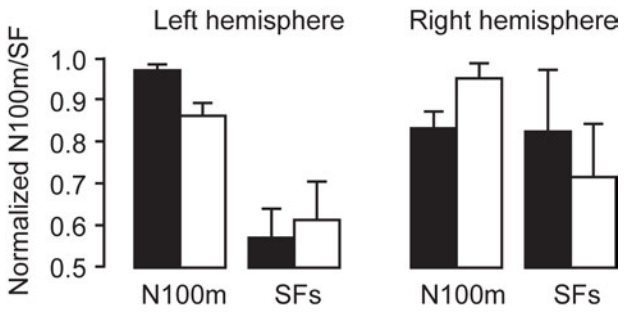


Figure 6. Normalized N100m and SF responses to dichotic tone pairs. Black bars indicate responses to the dichotic tone pair where the 400-Hz tone was presented to the LE and the 800-Hz tone to the RE, white bars indicate responses to the reversed tone pair. Modified from Study II.

5.2.2 Discussion

Monaural sounds elicit typically stronger N100m responses in the contralateral than the ipsilateral hemisphere (Hari, 1990). Thus, our results suggest that the hemispheric balance of the transient N100m responses follow the sound localization during the octave illusion. The results agree with the behavioural model, according to which the perceived locations follow the ear currently receiving the high tone.

5.3 Modified binaural interaction contributes to the peculiar pitch perception during the octave illusion (Study III)

Study II suggested that the auditory SFs may reflect the perceived pitches during dichotic tones one octave apart.

We aimed to investigate with a MEG-based frequency-tagging method (Fujiki et al., 2002) whether the modified binaural interaction between dichotic tones contributes to the pitch perception during the octave illusion. The method allows separation of cortical responses to each ear input during binaural listening.

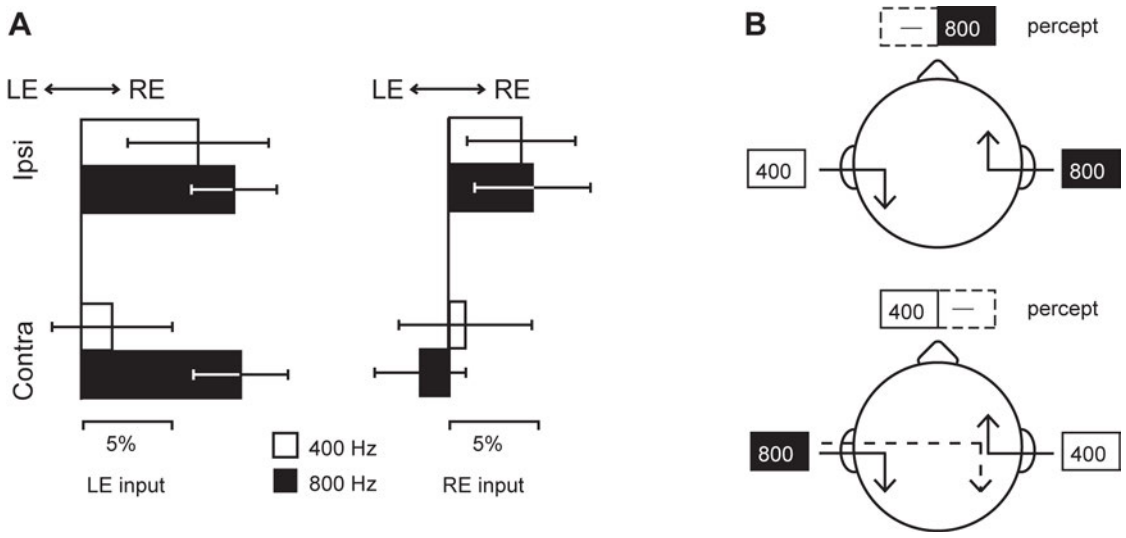


Figure 7. A) Ear-dominance. B) Neurophysiological model of pitch perception. Modified from Study III.

5.3.1 Results

After the preliminary behavioural study, we restricted our MEG analysis to subjects who perceived the octave illusion in the classical manner (Deutsch, 1974, 1983; Brennan and Stevens, 2002), i.e. the single high tones in the RE, alternating with a single low tones in the LE. The MEG results on ipsilateral suppressions demonstrated increased right-ear dominance for both tones of the dichotic sounds (Fig. 7A; for 400-Hz, p = 0.008; for 800-Hz, p = 0.004). In addition, during the dichotic stimulus corresponding to the most peculiar tone pair in the octave illusion, i.e when the

perceived source localization (LE) disagreed with the perceived pitch (frequency of RE tone), contralateral responses to LE tones also showed increased right-ear dominance (the lower part in Fig. 7A).

5.3.2 Discussion

The findings of our study demonstrate that binaural interaction contributes to the peculiar pitch perception during the octave illusion. In addition, the results highlight the possible different roles of ipsilateral and contralateral responses in binaural processing and auditory perception.

The increased RE-dominance agrees with the behavioural data about the octave illusion (Deutsch, 1975; Deutsch and Roll, 1976; Deutsch, 2004a). We suggested a tentative neurophysiological counterpart to the behavioural model (Fig. 7B): during both dichotic tone pairs, ipsilateral SSRs to the ignored LE-inputs decreased and to the perceived RE-inputs increased. In addition, when the LE received the 800-Hz tone and the RE the 400-Hz tone, but people typically perceive a low tone incorrectly in the LE during the illusion, also contralateral responses to the LE-inputs decreased.

5.4 Early cortical processing of natural sounds can be studied with amplitude-modulated speech and music (Study IV)

Neuromagnetic SSFs, elicited by amplitude modulated tones, have been successfully used to study binaural interaction both in healthy and dyslexic subjects (Fujiki et al., 2002; Kaneko et al., 2003; Study I). In addition, SSPs to modulated tones have been used in audiology diagnostics to quantify the frequency-specific hearing thresholds in infants and other non-co-operative patients (Picton et al., 2003).

In daily life, we hear much more complex auditory stimuli than tones, for example speech and music. Although defective binaural interaction in hearing-impaired patients has been suggested to be the underlying cause of problems in speech comprehension, frequency-specific hearing thresholds are often unable to estimate the problems in speech comprehension or music listening.

SSFs and the frequency-tagging method might provide a feasible way to study early cortical processing and binaural interaction of natural sounds. We therefore studied whether speech and music can elicit reliable SSFs and how the modulation changes the quality and naturalness of the sounds.

5.4.1 Results

The intelligibility of the speech and the musical quality of the stimuli worsened with increasing modulation depths (from 25% to 100%). However, all subjects still understood the contents of speech at all depths. The modulation deteriorated significantly more in music than in speech ($p < 0.003$).

The responses were the strongest to the tone stimuli and the weakest to speech stimuli. For all sounds (tones, music, speech), the responses diminished with decreasing modulation depth (Fig. 8). For most subjects, all tone stimuli and music modulated at 50–100% depths elicited clear SSFs and spectral peaks over both temporal lobes, whereas speech required 75% (or for some subjects even 100%) modulation depth (Fig.8).

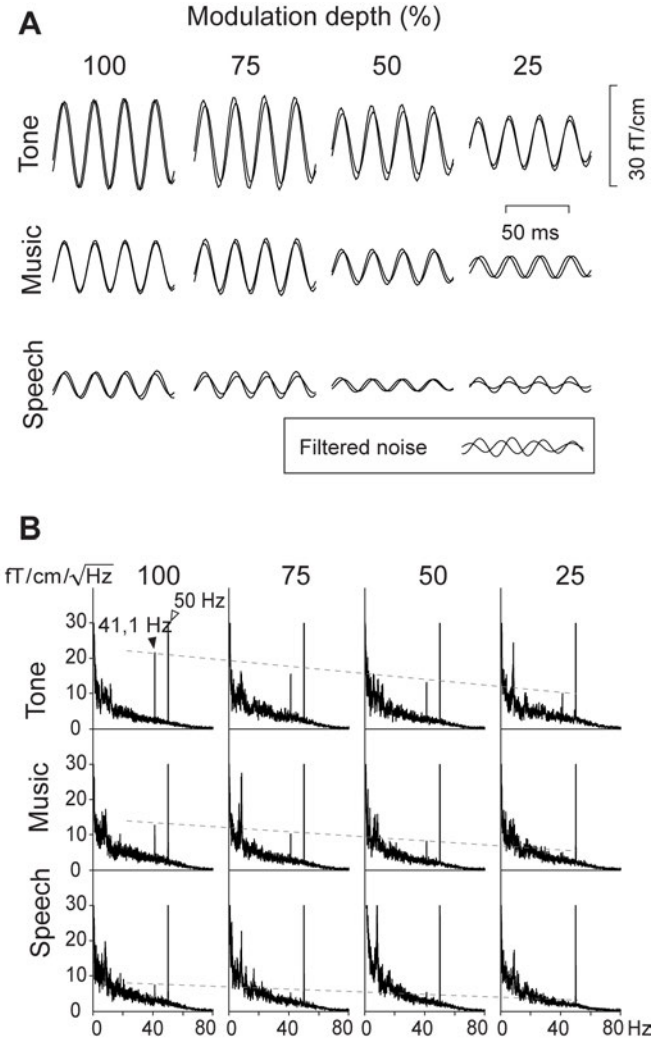


Figure 8. Auditory steady-state responses of a representative subject. A) Time-domain representation. B) Frequency-domain representation. Adapted from the submitted manuscript of Study IV.

5.4.2 Discussion

Our results demonstrate than natural, physically complex sounds, such as speech and music, can elicit reliable SSFs, and thus seem appropriate to use in further studies of healthy and diseased subjects.

According to effects of modulation depth on the sound quality and the response strengths, the 100% modulation depth might be the most feasible in studying processing of speech, whereas with music, the 75% or even 50% modulation depth might be a suitable compromise between the SNR of SSFs and perceptual fidelity.

6 General discussion

6.1 Connections between *ROBO1*, binaural processing, crossing of auditory pathways, and dyslexia

Until now, the neurodevelopmenral function and role of the human *ROBO1* gene have remained unclear, although it is suggested to predispose to dyslexia (Nopola-Hemmi et al., 2001; Fisher et al., 2002; Hannula-Jouppi et al., 2005) and shows linkage to autism (Anitha et al., 2008) and phonological processing (Bates et al., 2011). In addition, a region around the *ROBO1* gene has been associated with a speech sound disorder, an SLI-variant (Stein et al., 2004). The underlying causes of all these disorders—each of them relating at some level to language and auditory processing—are unknown.

Our results of impaired binaural interaction in *ROBO1*-deficient subjects revealed for the first time the significance of the *ROBO1* gene in sensory processing and brain function. The correlation between the binaural suppression and the expression level of *ROBO1* suggests that, for normal binaural processing, adequate expression level is needed. Studies in fruit flies and mice have demonstrated the critical roles of *robo* and *Robo1*, orthologs of human *ROBO1*, for axonal midline crossing during development (Kidd et al., 1998a; Kidd et al., 1998b; Brose et al., 1999; Andrews et al., 2006). Because binaural interaction requires axonal midline crossing—otherwise the inputs of the LE and the RE would not converge—and because normal auditory pathways show extensive crossing in the brain stem, the found impaired binaural interaction suggests defective crossing of auditory pathways. During embryonic development of the rat nervous system, *Robo1* mRNA has been found in many places around the auditory system (Marillat et al., 2002): in CNs and ICs, both sending crossing axons to the

opposite side (Moore, 1991), and in medial part of the dorsal thalamus and in lateral cortices. Above the tectum, the auditory pathways remain totally or near-totally ipsilateral, and therefore the defective crossing may take place already in the CNs or in the ICs. The ICs are one of the most important structures for binaural processing (Moore, 1991).

In our *ROBO1*-deficient subjects, dyslexia co-segregated with the *ROBO1* gene defect in a dominant manner. Dyslexia is a complex neurodevelopmental disorder with strong genetic background. Until now, six genes, *DYX1C1*, *DCDC2*, *KIAA0319*, *C2Orf3*, *MRPL19*, and *ROBO1* have been associated to dyslexia susceptibility (for a review, see Kere, 2011; Peterson and Pennington, 2012), and linkages to several additional genetic regions are weakly established (for a review, see Scerri and Schulte-Körne, 2010; Peterson and Pennington, 2012). Animal studies have clarified the roles of the *DYX1C1*, *DCDC2*, *KIAA0319*, and *ROBO1* in neuronal migration and axon guidance during embryonic development (for a review, see Galaburda et al., 2006; Scerri and Schulte-Körne, 2010; Kere, 2011), but they have not managed to bring knowledge about their role in sensory or any other neural processing.

Previous neuroimaging studies in healthy humans have associated *DYX1C1*, *DCDC2* and *KIAA0319*, but not *ROBO1*, to brain morphology. Specific polymorphisms of *DYX1C1*, *DCDC2*, and *KIAA0319* were associated with white matter density in left temporo-parietal area (Darki et al., 2012) and *DCDC2* genotypes were associated with grey matter volumes in superior, middle and inferior temporal gyri in the LH, and also with fusiform, hippocampal/para-hippocampal, inferior and middle frontal, and inferior occipito-temporal gyri in the LH (Meda et al., 2008). In an fMRI study, genetic variants of the *KIAA0319* locus were associated both with activation and hemispheric asymmetry of activation of posterior STS during reading (Pinel et al., 2012). Before the Study I, only one study of dyslexic subjects has examined the connections between the dyslexia candidate genes and neurophysiology: in German children, auditory late mismatch negativity (MMN), 400–600 ms after syllable onset, was associated with four specific variants in a genetic region containing *KIAA0319* and *DCDC2* (Czamara et al., 2011). Late MMN, on the other hand, has been suggested to be related to letter-speech integration (Froyen et al., 2009), and in dyslexic individuals late MMN amplitudes to speech stimuli have been small (Schulte-Körne et al., 2001).

Altogether, earlier data, and especially human data, about the functions of dyslexia susceptibility genes are sparse, and our result of strongly suppressed binaural interaction implying defective crossing of auditory pathways provides novel functional and anatomical knowledge about the interaction between the human sensory nervous system and dyslexia susceptibility gene. It remains unclear whether the found impairments in binaural processing parallel, contribute, or even cause some symptoms of dyslexia. Interestingly, in dyslexic subjects, enhancement of brainstem responses to repetitive speech sounds is abnormally weak and this enhancements correlates with speech understanding in noise (Chandrasekaran et al., 2009). On the other hand, speech perception is better with two ears than one ear, most probably because of binaural interaction (Cherry, 1953).

During the last decades, a variety of phonological, visual, auditory, attention, and tactile deficits have been found in dyslexic subjects and many different hypotheses of dyslexia have been suggested. Many of the found deficits may result from the defective function of certain dyslexia susceptibility genes, but are not necessarily causally related to the development of dyslexia. Interestingly, all studies of dyslexia candidate genes thus far have shown linkage to the temporal lobes. However, they have not managed to reveal the underlying brain functions and e.g. the role of auditory processing deficits in development of dyslexia remain unclear, although their possible causal role has been again highlighted (Galaburda et al., 2006; Goswami, 2011).

To show whether the impaired binaural interaction associates only with *ROBO1* gene expression or also with some other dyslexia susceptibility genes, comparisons between dyslexics with different genetic backgrounds might be informative. In Study I, no correlation analyses between the binaural interaction and *ROBO1* gene expression in healthy controls were carried out, although the controls showed wide individual variability in binaural interaction levels. Therefore, it remains unclear whether the *ROBO1* expression also correlates with binaural interaction in the general population. In future studies, the relationships between binaural interaction, different phonetic deficits, speech perception in background noise, and also sound localization ability may be clarified. In addition, studies of binaural interaction with speech sounds might provide further information about binaural processing. However, revealing—or proving to be

false—the possible link between the auditory deficit and later developmental defects is challenging. The central auditory system can undergo remarkable plastic changes and compensate for many disturbances; e.g. commissural pathways and association axons, the important connections between different auditory areas and thus to the perception of complex auditory stimuli, mature strongly during childhood and early adolescence (Moore, 2002), and reading ability, as any acquired skill, also modifies the brain (Dehaene et al., 2010). Thus, the original underlying defects may disappear or fade during development and may not be measurable in adults, whereas the other non-causal symptoms may even strengthen (Galaburda et al., 2006).

6.2 Binaural processing in the octave illusion

In some situations, auditory processing results in inaccurate sound interpretation. Associations between false percepts and the underlying abnormal condition, such as specific illusory sound stimuli or brain lesions, may provide valuable information about normal brain function (about lesion studies, see e.g. Clarke et al., 2000; Adriani et al., 2003; or a review by Stewart et al., 2006). In the octave illusion, both sound localization (where?) and sound identification (what?) are imperfect (Deutsch, 1974; Deutsch and Roll, 1976), together forming an illusory percept of monaural sounds switching from ear to ear. What and where components of sounds are processed in the brain in parallel streams (Clarke et al., 2000; Rauschecker and Tian, 2000; Anourova et al., 2001), but overlap and contribute to each other during early cortical processing (Griffiths and Warren, 2002; van der Zwaag et al., 2011). Therefore, the octave illusion is an interesting phenomenon to study neural what and where processing and possibly also interactions between these partially separate pathways.

Studies II and III demonstrated different behaviours and therefore probable different functional roles of transient N100m responses, SFs, and SSRs: in both hemispheres, N100m responses were stronger to bilateral 800-Hz than bilateral 400-Hz tones, whereas SFs and SSRs were stronger to 400-Hz than 800-Hz tones, in line with previous studies (Stapells et al., 1984; Kuwada et al., 1986; Rodriguez et al., 1986; Pantev et al., 1996; Ross et al., 2000).

During dichotic stimuli, corresponding to tone pairs in the octave illusion, the N100m responses were stronger in both hemispheres to the tone pair with the contralateral 800-Hz than the contralateral 400-Hz tone. Because N100m responses are stronger in the contralateral hemisphere during monaural listening (for a review, see Hari, 1990), the findings support the behavioural model (Deutsch and Roll, 1976; Deutsch, 2004a), according to which the sounds are localized to the ear receiving the 800-Hz tone. The found differences in source strength may result from different binaural interactions between LE 800-Hz and RE 400-Hz tones than between LE 400-Hz and RE 800-Hz tones, i.e. contralateral 800-Hz tone suppresses ipsilateral N100m responses more than contralateral 400-Hz tone.

According to a previous MEG-study, contralateral inputs suppress the N100m responses to ipsilateral input in the RH—the LH was not studied—when the frequencies are the same in both ears, but not during dichotic tones (Brancucci et al., 2004). However, in that study, the frequency difference between the dichotic tones was always less than one octave, and responses to harmonic 400-Hz and 800-Hz tones might behave somehow similarly than to tones with the same frequency. No N100m data about the possible different ipsilateral suppression elicited by contralateral 800-Hz rather than 400-Hz tones exist, but binaural suppression of ipsilateral SSRs tends to be stronger during binaural 800-Hz than 400-Hz tones ($p < 0.09$ in the LH, $p < 0.06$ in the RH; unpublished data). However, as pointed out, N100m responses and SSRs reflect different cortical processes and often behave differently, thus no straight conclusion can be drawn from SSRs to the N100m responses.

The other explanation for the N100m results of dichotic tones in Study II could be simple summation of responses to the LE and the RE inputs. According to results of Study II, N100m responses tended to be stronger to 800-Hz than 400-Hz tones, and on the other hand N100m responses are typically clearly stronger in the contralateral than the ipsilateral hemisphere during monaural stimulation (Pantev et al., 1998). Thus, N100m responses could be stronger to the dichotic tone pair with contralateral 800-Hz than contralateral 400-Hz tone, if the effects of other factors (such as lateralization, ear of stimulation, and hemisphere) are negligible. However, no data exist e.g. about lateralization of N100m responses to one ear input during binaural listening. Overall, it is not known, whether the dichotic tone pairs in general tend to be localized more towards the auditory space of higher tone or not.

Study III demonstrated that during both dichotic tones, ipsilateral SSRs in the LH were weaker and in the RH stronger than during binaural stimulation with the same frequency in both ears. Thus, contribution of the LE tones to the LH responses was weaker and contribution of the RE tones to the RH responses stronger during dichotic than binaural tones with the same input in both ears. In addition, contralateral responses to 800-Hz LE tones were weaker during dichotic than binaural same-pitch tones, meaning that the contribution of the LE tone to the RH responses were weaker during dichotic stimuli. Other contralateral responses showed no significant difference between the stimuli. Overall, ipsi- and contralateral differences between the stimuli can be interpreted as

stronger RE-dominance during dichotic stimuli. Therefore, the results of Study III match the behavioural model according to which perceived pitches follow the RE input (Deutsch, 1974; Deutsch and Roll, 1976; Deutsch, 2004a), and on the basis of results of the Studies II and III, a neurophysiological counterpart to the behavioural model was suggested in Study III.

The octave illusion requires an alternation of dichotic tones between the ears (Deutsch, 1974, 1988). Studies in this thesis showed that dichotic tones, without alternation, elicit specific cortical responses which we suggest are associated with the perceived locations and pitches during the illusion. Alternation, i.e. repetition of the tones, might force these responses during long stimulus sequences, but an additional streaming by ear, i.e organizing inputs into meaningful groups, may contribute to the illusory percepts. Along with the method development, studying the octave illusion with alternating stimuli by means of frequency tagging and categorizing the responses according to the different dichotic tone pairs appears to be feasible. Further, the percepts of the octave illusion typically differ between the left- and right-handed subjects (Deutsch, 1983), and in both groups, the percepts often change spontaneously during long sound sequences (Deutsch, 1974). Studies according to different percepts may provide further knowledge about “what” and “where” processes and possible interactions between them. However, analysis of the MEG data according to different percepts accurately and reliably is challenging; for visual responses such analysis has already been done successfully (Parkkonen et al., 2008).

6.3 Natural stimuli in studying early cortical processing and binaural interaction

In the early days of auditory functional neuroimaging, very simple sound stimuli, such as clicks or noise bursts, were used to evoke auditory responses and to study the strength and location of the activation. Over the last decades, more and more complex sounds have been increasingly used, and more recently, still more natural/naturalistic stimuli and experimental setups have been applied (see e.g. Baess et al., 2012; Koskinen et al., 2012).

Study IV demonstrated that natural sounds, speech and music, can be used as reliable carrier sounds to evoke SSFs. The tone stimuli generated the strongest responses and the speech stimuli, the physically the most complex stimuli, produced the weakest responses. Because the SNR improved with deepening modulation depth but the sound quality worsened simultaneously, sound parameters have to be selected carefully for each experiment. The results suggest that for speech studies, at least 75% or even 100% modulation depth is required, whereas in music studies, 50% modulation depth might be needed to retain sufficient sound quality. Because no spectrally and temporally matched non-speech or non-music stimuli were used, it remains unclear whether the found differences in SSRs to tones, music, and speech result from physical properties of the sound or information or both.

In clinical settings, SSRs have been used to evaluate frequency-specific hearing thresholds with amplitude- or frequency-modulated tones, or with a combination of them. Because many hearing problems are associated with problems in speech understanding and musical experience, SSRs evoked by natural sounds may in the future provide an important addition to diagnostic tools. However, before that the normal variation of SSRs to different sounds in different age groups has to be clarified. Moreover, the relationship between speech understanding and the SSRs to speech has to be examined.

Thus far, only pure tones have been used in studying binaural interaction in detail by the frequency-tagging method, so no data about SSRs to monaural/binaural natural sounds

exist. Study IV suggests that in the future, natural stimuli with carefully selected sound parameters may be used to study cortical auditory processing. Although frequency tagging has been used only with MEG, it might be applicable to EEG as well. Nowadays, EEG is much more easily accessible and therefore better suited to clinical circumstances.

6.4 Binaural interaction: clinical aspects

The current findings of the studies of this thesis also have clinical implications. For example, unilateral cochlear implant users have difficulties in detecting speech in noisy environments, but the performance of bilaterally implanted people is clearly improved (for a review, see Basura et al., 2009; or Ramsden et al., 2012). In addition, bilateral implantation improves the sound localization: although the spatial detection based on ITDs is still very weak, the ILD-based localization is even better than in healthy controls (Aronoff et al., 2012). However, most of the cochlear implant users in the world (over 44000 children and over 150000 adults; Peters et al., 2010; Ramsden et al., 2012) have unilateral implants, and most new candidates are provided only one implant (Ramsden et al., 2012). Currently, it is not clear how much the impairments in speech understanding and spatial detection result from defective binaural interaction, the underlying disease possibly affecting the ears differently, and/or the limitations of the devices, for example lack of optimization for binaural processing. In the future, SSRs to natural sounds and EEG-based frequency-tagging, if feasible, might provide new tools to study auditory processing, binaural interactions, and plasticity of the auditory system in cochlear implant users.

Presbyacusia, the most common form of hearing loss affecting older adults, is caused by the gradual loss of high frequency sensitivity. For many patients, the most disturbing symptom, however, is the difficulty in understanding speech in background noise and in reverberating environments. Speech understanding problems have been explained by peripheral deficits, but central problems in binaural interaction have also been suggested (Frisina and Frisina, 1997; Martin and Jerger, 2005).

In general, the patient's ability to understand speech can be estimated from the pure-tone audiogram, but in many cases this will provide wrong results about the overall performance, and more detailed clinical tests of speech and binaural processing have been demanded (Wilson and McArdle, 2005).

7 Conclusion

This thesis revealed the neurodevelopmental function of the human *ROBO1* gene by demonstrating defective binaural interaction and thus weak midline crossing of auditory pathways in individuals with *ROBO1* gene deficit. The results of Study I link human *ROBO1*, and also any dyslexia susceptibility gene, for the first time to a deficit in sensory processing, and to any specific neural mechanisms of human brain.

Studies II and III demonstrated the neural correlates of peculiar sound localization and pitch perception during the octave illusion. Transient N100m responses, typically stronger in the hemisphere contralateral to the stimulated ear, followed the perceived locations (the ear actually receiving the higher frequency tone). During dichotic tones corresponding to the octave illusion, the RE dominance increased, as the result of modified binaural interaction. On the basis of results of Studies II and III, a tentative neurophysiological counterpart to the behavioural model was suggested: the N100m responses follow the higher frequency and the sound localization, whereas SSRs follow the RE, and thus the perceived pitches.

According to the results of Study IV, natural sounds such as speech and music, can be used to elicit reliable SSRs, suggesting that, in the future, it is feasible to study early cortical processing and binaural interaction with natural sounds.

References

Adriani M, Bellmann A, Meuli R, Fornari E, Frischknecht R, Bindschaedler C, Rivier F, Thiran JP, Maeder P, and Clarke S. Unilateral hemispheric lesions disrupt parallel processing within the contralateral intact hemisphere: an auditory fMRI study. *Neuroimage* 2003, 20 Suppl 1: S66–74.

Ahissar M. Dyslexia and the anchoring-deficit hypothesis. *Trends Cogn Sci* 2007, 11: 458–465.

Ahonen AI, Hämäläinen MS, Kajola MJ, Knuutila JET, Laine PP, Lounasmaa OV, Parkkonen L, Simola JT, and Tesche CD. 122-Channel SQUID instrument for investigating the magnetic signals from the human brain *Physica Scripta* 1993, T49: 198–205.

Ahveninen J, Jääskeläinen IP, Raij T, Bonmassar G, Devore S, Hämäläinen M, Levänen S, Lin FH, Sams M, Shinn-Cunningham BG, Witzel T, and Belliveau JW. Task-modulated "what" and "where" pathways in human auditory cortex. *Proc Natl Acad Sci U S A* 2006, 103: 14608–14613.

Andrews W, Liapi A, Plachez C, Camurri L, Zhang J, Mori S, Murakami F, Parnavelas JG, Sundaresan V, and Richards LJ. Robo1 regulates the development of major axon tracts and interneuron migration in the forebrain. *Development* 2006, 133: 2243–2252.

Anitha A, Nakamura K, Yamada K, Suda S, Thanseem I, Tsujii M, Iwayama Y, Hattori E, Toyota T, Miyachi T, Iwata Y, Suzuki K, Matsuzaki H, Kawai M, Sekine Y, Tsuchiya K, Sugihara G, Ouchi Y, Sugiyama T, Koizumi K, Higashida H, Takei N, Yoshikawa T, and Mori N. Genetic analyses of roundabout (*ROBO*) axon guidance receptors in autism. *Am J Med Genet B Neuropsychiatr Genet* 2008, 147B: 1019–1027.

Anogianakis G, Badier JM, Barrett G, Erné S, Fenici R, Fenwick P, Grandori F, Hari R, Ilmoniemi R, Mauguière F, Lehmann D, Perrin F, Peters M, Romani G-L, and Rossini PM. A consensus statement on relative merits of EEG and MEG. *Electroencephalogr Clin Neurophysiol* 1992, 82: 317–319.

Anourova I, Nikouline VV, Ilmoniemi RJ, Hotta J, Aronen HJ, and Carlson S. Evidence for dissociation of spatial and nonspatial auditory information processing. *Neuroimage* 2001, 14: 1268–1277.

Antervo A, Hari R, Katila T, Ryhänen T, and Seppänen M. Magnetic fields produced by eye blinking. *Electroencephalogr Clin Neurophysiol* 1985, 61: 247–253.

Aronoff JM, Freed DJ, Fisher LM, Pal I, and Soli SD. Cochlear implant patients' localization using interaural level differences exceeds that of untrained normal hearing listeners. *J Acoust Soc Am* 2012, 131: EL382–387.

Baess P, Zhdanov A, Mandel A, Parkkonen L, Hirvenkari L, Mäkelä JP, Jousmäki V, and Hari R. MEG dual scanning: a procedure to study real-time auditory interaction between two persons. *Front Hum Neurosci* 2012, 6: 83.

Bak CK, Lebech J, and Saermark K. Dependence of the auditory evoked magnetic field (100 msec signal) of the human brain on the intensity of the stimulus. *Electroencephalogr Clin Neurophysiol* 1985, 61: 141–149.

Basura GJ, Eapen R, and Buchman CA. Bilateral cochlear implantation: current concepts, indications, and results. *Laryngoscope* 2009, 119: 2395–2401.

Bates TC, Luciano M, Medland SE, Montgomery GW, Wright MJ, and Martin NG. Genetic variance in a component of the language acquisition device: *ROBO1* polymorphisms associated with phonological buffer deficits. *Behav Genet* 2011, 41: 50–57.

Brancucci A, Babiloni C, Babiloni F, Galderisi S, Mucci A, Tecchio F, Zappasodi F, Pizzella V, Romani GL, and Rossini PM. Inhibition of auditory cortical responses to ipsilateral stimuli during dichotic listening: evidence from magnetoencephalography. *Eur J Neurosci* 2004, 19: 2329–2336.

Brancucci A, Padulo C, and Tommasi L. "Octave illusion" or "Deutsch's illusion"? *Psychol Res* 2009, 73: 303–307.

Brennan D and Stevens C. Specialist musical training and the octave illusion: analytical listening and veridical perception by pipe organists. *Acta Psychol (Amst)* 2002, 109: 301–314.

Brennan SK, Brooke RE, and Stevens JC. The effect of varying stimulus phase between frequency and amplitude modulation on auditory steady-state responses in neonates. *Int J Audiol* 2012, 51: 116–123.

Brodmann K. *Vergleichende Localisationslehre der Grosshirnrinde in ihren Principien dargestellt auf Grund des Zellenbaues*. 1909. Leipzig: Johann Ambrosius Barth.

Brose K, Bland KS, Wang KH, Arnott D, Henzel W, Goodman CS, Tessier-Lavigne M, and Kidd T. Slit proteins bind Robo receptors and have an evolutionarily conserved role in repulsive axon guidance. *Cell* 1999, 96: 795–806.

Canale A, Lacilla M, Cavalot AL, and Albera R. Auditory steady-state responses and clinical applications. *Eur Arch Otorhinolaryngol* 2006, 263: 499–503.

Chambers CD, Mattingley JB, and Moss SA. Does selective attention influence the octave illusion? *Perception* 2005, 34: 217–229.

Chandrasekaran B, Hornickel J, Skoe E, Nicol T, and Kraus N. Context-dependent encoding in the human auditory brainstem relates to hearing speech in noise: implications for developmental dyslexia. *Neuron* 2009, 64: 311–319.

Cherry E. Some experiments on the recognition of speech, with one or with two ears. *J Acoust Soc Am* 1953, 25: 975–979.

Cherry R and Rubinstein A. Comparing monotic and diotic selective auditory attention abilities in children. *Lang Speech Hear Serv Sch* 2006, 37: 137–142.

Clark K, Hammond E, and Rabbitts P. Temporal and spatial expression of two isoforms of the Dutt1/Robo1 gene in mouse development. *FEBS Lett* 2002, 523: 12–16.

Clarke S, Bellmann A, Meuli RA, Assal G, and Steck AJ. Auditory agnosia and auditory spatial deficits following left hemispheric lesions: evidence for distinct processing pathways. *Neuropsychologia* 2000, 38: 797–807.

Clarke S and Rivier F. Compartments within human primary auditory cortex: evidence from cytochrome oxidase and acetylcholinesterase staining. *Eur J Neurosci* 1998, 10: 741–745.

Cohen D. Magnetoencephalography: evidence of magnetic fields produced by alpha-rhythm currents. *Science* 1968, 161: 784–786.

Cohen D. Magnetoencephalography: detection of the brain's electrical activity with a superconducting magnetometer. *Science* 1972, 175: 664–666.

Cohen D and Cuffin BN. Demonstration of useful differences between magnetoencephalogram and electroencephalogram. *Electroencephalogr Clin Neurophysiol* 1983, 56: 38–51.

Craig JD. The effects of musical training and cerebral asymmetries on perception of an auditory illusion. *Cortex* 1979, 15: 671–677.

Cuffin BN and Cohen D. Comparison of the magnetoencephalogram and electroencephalogram. *Electroencephalogr Clin Neurophysiol* 1979, 47: 132–146.

Czamara D, Bruder J, Becker J, Bartling J, Hoffmann P, Ludwig KU, Müller-Myhsok B, and Schulte-Körne G. Association of a rare variant with mismatch negativity in a region between KIAA0319 and DCDC2 in dyslexia. *Behav Genet* 2011, 41: 110–119.

Da Costa S, van der Zwaag W, Marques JP, Frackowiak RS, Clarke S, and Saenz M. Human primary auditory cortex follows the shape of Heschl's gyrus. *J Neurosci* 2011, 31: 14067–14075.

Darki F, Peyrard-Janvid M, Matsson H, Kere J, and Klingberg T. Three dyslexia susceptibility genes, DYX1C1, DCDC2, and KIAA0319, affect temporo-parietal white matter structure. *Biol Psychiatry* 2012: 1–6.

Dehaene S, Pegado F, Braga LW, Ventura P, Nunes Filho G, Jobert A, Dehaene-Lambertz G, Kolinsky R, Morais J, and Cohen L. How learning to read changes the cortical networks for vision and language. *Science* 2010, 330: 1359–1364.

Delb W, Strauss DJ, Hohenberg G, and Plinkert PK. The binaural interaction component (BIC) in children with central auditory processing disorders (CAPD). *Int J Audiol* 2003, 42: 401–412.

Deutsch D. An auditory illusion. *Nature* 1974, 251: 307–309.

Deutsch D. Two-channel listening to musical scales. *J Acoust Soc Am* 1975, 57: 1156–1160.

Deutsch D. The octave illusion in relation to handedness and familial handedness background. *Neuropsychologia* 1983, 21: 289–293.

Deutsch D. Lateralization and sequential relationships in the octave illusion. *J Acoust Soc Am* 1988, 83: 365–369.

Deutsch D. The octave illusion revisited again. *J Exp Psychol Hum Percept Perform* 2004a, 30: 355–364.

Deutsch D. Reply to "Reconsidering evidence for the suppression model of the octave illusion," by C. D. Chambers, J. B. Mattingley, and S. A. Moss. *Psychon Bull Rev* 2004b, 11: 667–676.

Deutsch D and Roll PL. Separate "what" and "where" decision mechanisms in processing a dichotic tonal sequence. *J Exp Psychol Hum Percept Perform* 1976, 2: 23–29.

Dobie RA and Berlin CI. Binaural interaction in brainstem-evoked responses. *Arch Otolaryngol* 1979, 105: 391–398.

Elberling C, Bak C, Kofoed B, Lebech J, and Saermark K. Magnetic auditory responses from the human brain. A preliminary report. *Scand Audiol* 1980, 9: 185–190.

Elberling C, Bak C, Kofoed B, Lebech J, and Saermark K. Auditory magnetic fields from the human cortex. Influence of stimulus intensity. *Scand Audiol* 1981, 10: 203–207.

Elberling C, Bak C, Kofoed B, Lebech J, and Saermark K. Auditory magnetic fields from the human cerebral cortex: location and strength of an equivalent current dipole. *Acta Neurol Scand* 1982, 65: 553–569.

Fisher SE, Francks C, Marlow AJ, MacPhie IL, Newbury DF, Cardon LR, Ishikawa-Brush Y, Richardson AJ, Talcott JB, Gayan J, Olson RK, Pennington BF, Smith SD, DeFries JC, Stein JF, and Monaco AP. Independent genome-wide scans identify a chromosome 18 quantitative-trait locus influencing dyslexia. *Nat Genet* 2002, 30: 86–91.

Formisano E, Kim DS, Di Salle F, van de Moortele PF, Ugurbil K, and Goebel R. Mirror-symmetric tonotopic maps in human primary auditory cortex. *Neuron* 2003, 40: 859–869.

Frisina DR and Frisina RD. Speech recognition in noise and presbycusis: relations to possible neural mechanisms. *Hear Res* 1997, 106: 95–104.

Froyen DJ, Bonte ML, van Atteveldt N, and Blomert L. The long road to automation: neurocognitive development of letter-speech sound processing. *J Cogn Neurosci* 2009, 21: 567–580.

Fuchs M, Wagner M, Wischmann HA, Kohler T, Theissen A, Drenckhahn R, and Buchner H. Improving source reconstructions by combining bioelectric and biomagnetic data. *Electroencephalogr Clin Neurophysiol* 1998, 107: 93–111.

Fujiki N, Jousmäki V, and Hari R. Neuromagnetic responses to frequency-tagged sounds: a new method to follow inputs from each ear to the human auditory cortex during binaural hearing. *J Neurosci* 2002, 22: RC205.

Fullerton BC and Pandya DN. Architectonic analysis of the auditory-related areas of the superior temporal region in human brain. *J Comp Neurol* 2007, 504: 470–498.

Furey ML, Tanskanen T, Beauchamp MS, Avikainen S, Uutela K, Hari R, and Haxby JV. Dissociation of face-selective cortical responses by attention. *Proc Natl Acad Sci U S A* 2006, 103: 1065–1070.

Galaburda A and Sanides F. Cytoarchitectonic organization of the human auditory cortex. *J Comp Neurol* 1980, 190: 597–610.

Galaburda AM, LoTurco J, Ramus F, Fitch RH, and Rosen GD. From genes to behavior in developmental dyslexia. *Nat Neurosci* 2006, 9: 1213–1217.

Galambos R, Makeig S, and Talmachoff PJ. A 40-Hz auditory potential recorded from the human scalp. *Proc Natl Acad Sci U S A* 1981, 78: 2643–2647.

Godey B, Schwartz D, de Graaf JB, Chauvel P, and Liégeois-Chauvel C. Neuromagnetic source localization of auditory evoked fields and intracerebral evoked potentials: a comparison of data in the same patients. *Clin Neurophysiol* 2001, 112: 1850–1859.

Goswami U. A temporal sampling framework for developmental dyslexia. *Trends Cogn Sci* 2011, 15: 3–10.

Griffiths TD. The neural processing of complex sounds. *Ann N Y Acad Sci* 2001, 930: 133–142.

Griffiths TD and Warren JD. The planum temporale as a computational hub. *Trends Neurosci* 2002, 25: 348–353.

Grothe B, Pecka M, and McAlpine D. Mechanisms of sound localization in mammals. *Physiol Rev* 2010, 90: 983–1012.

Gutschalk A, Hämäläinen MS, and Melcher JR. BOLD responses in human auditory cortex are more closely related to transient MEG responses than to sustained ones. *J Neurophysiol* 2010, 103: 2015–2026.

Gutschalk A, Mase R, Roth R, Ille N, Rupp A, Hahnel S, Picton TW, and Scherg M. Deconvolution of 40 Hz steady-state fields reveals two overlapping source activities of the human auditory cortex. *Clin Neurophysiol* 1999, 110: 856–868.

Gutschalk A and Uppenkamp S. Sustained responses for pitch and vowels map to similar sites in human auditory cortex. *Neuroimage* 2011, 56: 1578–1587.

Habib M. The neurological basis of developmental dyslexia: an overview and working hypothesis. *Brain* 2000, 123 Pt 12: 2373–2399.

Hackett TA, Preuss TM, and Kaas JH. Architectonic identification of the core region in auditory cortex of macaques, chimpanzees, and humans. *J Comp Neurol* 2001, 441: 197–222.

Hannula-Jouppi K, Kaminen-Ahola N, Taipale M, Eklund R, Nopola-Hemmi J, Kääriäinen H, and Kere J. The axon guidance receptor gene *ROBO1* is a candidate gene for developmental dyslexia. *PLoS Genet* 2005, 1: e50.

Hari R. The neuromagnetic method in the study of the human auditory cortex. In Grandori F, Hoke, M., Romani, GL. (Ed.) *Auditory Evoked Magnetic Fields and Electric Potentials. Advances in Audiology*, 1990. Basel: S. Karger, pp. 222–282.

Hari R. Magnetoencephalography in clinical neurophysiological assessment of human cortical functions. In Neidermeyer E, Lopes Da Silva, F. (Ed.) *Electroencephalography: Basic Principles, Clinical Applications, and Related Fields, 5th edition*, 2004. Baltimore: Williams and Wilkins, pp. 1165–1197.

Hari R, Aittoniemi K, Järvinen ML, Katila T, and Varpula T. Auditory evoked transient and sustained magnetic fields of the human brain. Localization of neural generators. *Exp Brain Res* 1980, 40: 237–240.

Hari R, Hämäläinen M, Ilmoniemi R, Kaukoranta E, Reinikainen K, Salminen J, Alho K, Näätänen R, and Sams M. Responses of the primary auditory cortex to pitch changes in a sequence of tone pips: neuromagnetic recordings in man. *Neurosci Lett* 1984, 50: 127–132.

Hari R, Hämäläinen M, and Joutsiniemi SL. Neuromagnetic steady-state responses to auditory stimuli. *J Acoust Soc Am* 1989a, 86: 1033–1039.

Hari R, Hämäläinen M, Kaukoranta E, Mäkelä J, Joutsiniemi SL, and Tiihonen J. Selective listening modifies activity of the human auditory cortex. *Exp Brain Res* 1989b, 74: 463–470.

Hari R, Kaila K, Katila T, Tuomisto T, and Varpula T. Interstimulus interval dependence of the auditory vertex response and its magnetic counterpart: implications for their neural generation. *Electroencephalogr Clin Neurophysiol* 1982, 54: 561–569.

Hari R and Kiesilä P. Deficit of temporal auditory processing in dyslexic adults. *Neurosci Lett* 1996, 205: 138–140.

Hari R, Levänen S, and Raij T. Timing of human cortical functions during cognition: role of MEG. *Trends Cogn Sci* 2000, 4: 455–462.

Hari R and Lounasmaa OV. Recording and interpretation of cerebral magnetic fields. *Science* 1989, 244: 432–436.

Hari R and Mäkelä JP. Modification of neuromagnetic responses of the human auditory cortex by masking sounds. *Exp Brain Res* 1988, 71: 87–92.

Hari R, Pelizzone M, Mäkelä JP, Hällstrom J, Leinonen L, and Lounasmaa OV. Neuromagnetic responses of the human auditory cortex to on- and offsets of noise bursts. *Audiology* 1987, 26: 31–43.

Hari R, Pelizzone M, Mäkelä JP, Hällström J, Huttunen J, and Knuutila J. Neuromagnetic responses from a deaf subject to stimuli presented through a multichannel cochlear prosthesis. *Ear Hear* 1988, 9: 148–152.

Hari R and Renvall H. Impaired processing of rapid stimulus sequences in dyslexia. *Trends Cogn Sci* 2001, 5: 525–532.

Hari R and Salmelin R. Magnetoencephalography: From SQUIDs to neuroscience Neuroimage 20th Anniversary Special Edition. *Neuroimage* 2012.

Hari R, Sääskilahti A, Helenius P, and Uutela K. Non-impaired auditory phase locking in dyslexic adults. *Neuroreport* 1999, 10: 2347–2348.

Helenius P, Salmelin R, Richardson U, Leinonen S, and Lyytinen H. Abnormal auditory cortical activation in dyslexia 100 msec after speech onset. *J Cogn Neurosci* 2002, 14: 603–617.

Helenius P, Uutela K, and Hari R. Auditory stream segregation in dyslexic adults. *Brain* 1999, 122 (Pt 5): 907–913.

Hinshelwood J. A case of dyslexia: A peculiar form of word-blindness. *Lancet* 1896, 148: 1451–1454.

Hinshelwood J. A case of "word" without "letter" blindness. *Lancet* 1898, 151: 422–425.

Hinshelwood J. Two Cases of Hereditary Congenital Word-Blindness. *Br Med J* 1911, 1: 608–609.

Humphries C, Liebenthal E, and Binder JR. Tonotopic organization of human auditory cortex. *Neuroimage* 2010, 50: 1202–1211.

Hämäläinen M. Anatomical correlates for magnetoencephalography: integration with magnetic resonance images. *Clin Phys Physiol Meas* 1991, 12 Suppl A: 29–32.

Hämäläinen M, Hari R, Ilmoniemi RJ, Knuutila J, and Lounasmaa OV. Magnetoencephalography – theory, instrumentation, and applications to noninvasive studies of the working human brain. *Reviews of Modern Physics* 1993, 65: 413–497.

Hämäläinen MS and Sarvas J. Realistic conductivity geometry model of the human head for interpretation of neuromagnetic data. *IEEE Trans Biomed Eng* 1989, 36: 165–171.

Imig TJ and Brugge JF. Sources and terminations of callosal axons related to binaural and frequency maps in primary auditory cortex of the cat. *J Comp Neurol* 1978, 182: 637–660.

Imig TJ and Morel A. Organization of the thalamocortical auditory system in the cat. *Annu Rev Neurosci* 1983, 6: 95–120.

Imig TJ and Reale RA. Ipsilateral corticocortical projections related to binaural columns in cat primary auditory cortex. *J Comp Neurol* 1981, 203: 1–14.

John MS, Brown DK, Muir PJ, and Picton TW. Recording auditory steady-state responses in young infants. *Ear Hear* 2004, 25: 539–553.

Johnson MB, Kawasawa YI, Mason CE, Krsnik Z, Coppola G, Bogdanovic D, Geschwind DH, Mane SM, State MW, and Sestan N. Functional and evolutionary insights into human brain development through global transcriptome analysis. *Neuron* 2009, 62: 494–509.

Johnston JC, Durieux-Smith A, Angus D, O'Connor A, and Fitzpatrick E. Bilateral paediatric cochlear implants: a critical review. *Int J Audiol* 2009, 48: 601–617.

Kaas JH and Hackett TA. 'What' and 'where' processing in auditory cortex. *Nat Neurosci* 1999, 2: 1045–1047.

Kaas JH and Hackett TA. Subdivisions of auditory cortex and processing streams in primates. *Proc Natl Acad Sci U S A* 2000, 97: 11793–11799.

Kajola M, Ahonen A, Hämäläinen MS, Knuutila J, Lounasmaa OV, Simola J, and Vilkman V. Development of multichannel neuromagnetic instrumentation in Finland. *Clin Phys Physiol Meas* 1991, 12 Suppl B: 39–44.

Kandel E, Schwartz J, and Jessell T. *Principles in Neural Science, Fourth Edition* 2004: WcGeaw-Hill.

Kandler K, Clause A, and Noh J. Tonotopic reorganization of developing auditory brainstem circuits. *Nat Neurosci* 2009, 12: 711–717.

Kaneko K, Fujiki N, and Hari R. Binaural interaction in the human auditory cortex revealed by neuromagnetic frequency tagging: no effect of stimulus intensity. *Hear Res* 2003, 183: 1–6.

Keceli S, Inui K, Okamoto H, Otsuru N, and Kakigi R. Auditory sustained field responses to periodic noise. *BMC Neurosci* 2012, 13: 1–7.

Kere J. Molecular genetics and molecular biology of dyslexia. *Wiley Interdisciplinary Reviews: Cognitive Science* 2011, 2: 441–448.

Kidd T, Bland KS, and Goodman CS. Slit is the midline repellent for the robo receptor in *Drosophila*. *Cell* 1999, 96: 785–794.

Kidd T, Brose K, Mitchell KJ, Fetter RD, Tessier-Lavigne M, Goodman CS, and Tear G. Roundabout controls axon crossing of the CNS midline and defines a novel subfamily of evolutionarily conserved guidance receptors. *Cell* 1998a, 92: 205–215.

Kidd T, Russell C, Goodman CS, and Tear G. Dosage-sensitive and complementary functions of roundabout and commissureless control axon crossing of the CNS midline. *Neuron* 1998b, 20: 25–33.

Knuutila JET, Ahonen AI, Hämäläinen MS, Kajola MJ, Laine PP, Lounasmaa OV, Parkkonen L, Simola JT, and Tesche CD. 122-Channel whole-cortex SQUID system for measuring the brain's magnetic fields *IEEE Trans Magn* 1993, 29: 3315–3320.

Koskinen M, Viinikanoja J, Kurimo M, Klami A, Kaski S, and Hari R. Identifying fragments of natural speech from the listener's MEG signals. *Hum Brain Mapp* 2012: epub ahead of print.

Kuriki S, Nogai T, and Hirata Y. Cortical sources of middle latency responses of auditory evoked magnetic field. *Hear Res* 1995, 92: 47–51.

Kuwada S, Batra R, and Maher VL. Scalp potentials of normal and hearing-impaired subjects in response to sinusoidally amplitude-modulated tones. *Hear Res* 1986, 21: 179–192.

Leonard CM, Puranik C, Kuldau JM, and Lombardino LJ. Normal variation in the frequency and location of human auditory cortex landmarks. Heschl's gyrus: where is it? *Cereb Cortex* 1998, 8: 397–406.

Liegeois-Chauvel C, Musolino A, and Chauvel P. Localization of the primary auditory area in man. *Brain* 1991, 114 (Pt 1A): 139–151.

Liljeström M, Hulten A, Parkkonen L, and Salmelin R. Comparing MEG and fMRI views to naming actions and objects. *Hum Brain Mapp* 2009, 30: 1845–1856.

Lin YH, Chen PR, Hsu CJ, and Wu HP. Validation of multi-channel auditory steady-state response in adults with sensorineural hearing loss. *J Laryngol Otol* 2009, 123: 38–44.

Lyytinen H, Leinonen S, Nikula M, Aro M, and Leiwo M. In search of the core features of dyslexia: Observations concerning dyslexia in the highly orthographically regular Finnish language. In Berninger V (Ed.) *The Varieties of Orthographic Knowledge II: Relationships to Phonology, Reading, and Writing.* , 1995. Dordrecht, The Netherlands: Kluwer Academic Publishers, pp. 177–204.

Marillat V, Cases O, Nguyen-Ba-Charvet KT, Tessier-Lavigne M, Sotelo C, and Chedotal A. Spatiotemporal Expression Patterns of *slit* and *robo* Genes in the Rat Brain. *J Comp Neurol* 2002, 442: 130–155.

Martin JS and Jerger JF. Some effects of aging on central auditory processing. *J Rehabil Res Dev* 2005, 42: 25–44.

McArdle RA, Killion M, Mennite MA, and Chisolm TH. Are two ears not better than one? *J Am Acad Audiol* 2012, 23: 171–181.

McEvoy L, Mäkelä JP, Hämäläinen M, and Hari R. Effect of interaural time differences on middle-latency and late auditory evoked magnetic fields. *Hear Res* 1994, 78: 249–257.

Meda SA, Gelernter J, Gruen JR, Calhoun VD, Meng H, Cope NA, and Pearlson GD. Polymorphism of DCDC2 reveals differences in cortical morphology of healthy individuals-a preliminary voxel based morphometry study. *Brain Imaging Behav* 2008, 2: 21–26.

Moore DR. Anatomy and physiology of binaural hearing. *Audiology* 1991, 30: 125–134.

Moore JK. Maturation of human auditory cortex: implications for speech perception. *Ann Otol Rhinol Laryngol Suppl* 2002, 189: 7–10.

Morgan WP. A case of congenital word blindness. *Br Med J* 1896, 2: 1378.

Morosan P, Rademacher J, Schleicher A, Amunts K, Schormann T, and Zilles K. Human primary auditory cortex: cytoarchitectonic subdivisions and mapping into a spatial reference system. *Neuroimage* 2001, 13: 684–701.

Murakami S and Okada Y. Contributions of principal neocortical neurons to magnetoencephalography and electroencephalography signals. *J Physiol* 2006, 575: 925–936.

Mäkelä JP, Ahonen A, Hämäläinen M, Hari R, Ilmoniemi RJ, Kajola M, Knuutila J, Lounasmaa OV, McEvoy L, Salmelin R, Salonen O, Sams M, Simola J, Tesche C, and Vasama J-P. Functional differences between auditory cortices of the two hemispheres revealed by whole-head neuromagnetic recordings *Human Brain Mapping* 1993, 1: 48–56.

Mäkelä JP and Hari R. Evidence for cortical origin of the 40 Hz auditory evoked response in man. *Electroencephalogr Clin Neurophysiol* 1987, 66: 539–546.

Mäkelä JP and Hari R. Long-latency auditory evoked magnetic fields. *Adv Neurol* 1990, 54: 177–191.

Mäkelä JP and Hari R. Neuromagnetic auditory evoked responses after a stroke in the right temporal lobe. *Neuroreport* 1992, 3: 94–96.

Mäkelä JP, Hari R, Valanne L, and Ahonen A. Auditory evoked magnetic fields after ischemic brain lesions. *Ann Neurol* 1991, 30: 76–82.

Mäkelä JP, Hämäläinen M, Hari R, and McEvoy L. Whole-head mapping of middle-latency auditory evoked magnetic fields. *Electroencephalogr Clin Neurophysiol* 1994, 92: 414–421.

Nangini C, Hlushchuk Y, and Hari R. Predicting stimulus-rate sensitivity of human somatosensory fMRI signals with MEG. *Hum Brain Mapp* 2009, 30: 1824–1832.

Nopola-Hemmi J, Myllyluoma B, Haltia T, Taipale M, Ollikainen V, Ahonen T, Voutilainen A, Kere J, and Widen E. A dominant gene for developmental dyslexia on chromosome 3. *J Med Genet* 2001, 38: 658–664.

Nopola-Hemmi J, Myllyluoma B, Voutilainen A, Leinonen S, Kere J, and Ahonen T. Familial dyslexia: neurocognitive and genetic correlation in a large Finnish family. *Dev Med Child Neurol* 2002, 44: 580–586.

Nural HF, Todd Farmer W, and Mastick GS. The Slit receptor *Robo1* is predominantly expressed via the *Dutt1* alternative promoter in pioneer neurons in the embryonic mouse brain and spinal cord. *Gene Expr Patterns* 2007, 7: 837–845.

Ojima H. Interplay of excitation and inhibition elicited by tonal stimulation in pyramidal neurons of primary auditory cortex. *Neurosci Biobehav Rev* 2011, 35: 2084–2093.

Okada YC, Wu J, and Kyuhou S. Genesis of MEG signals in a mammalian CNS structure. *Electroencephalogr Clin Neurophysiol* 1997, 103: 474–485.

Pantev C, Hoke M, Lehnertz K, Lütkenhoner B, Anogianakis G, and Wittkowski W. Tonotopic organization of the human auditory cortex revealed by transient auditory evoked magnetic fields. *Electroencephalogr Clin Neurophysiol* 1988, 69: 160–170.

Pantev C, Lütkenhöner B, Hoke M, and Lehnertz K. Comparison between simultaneously recorded auditory-evoked magnetic fields and potentials elicited by ipsilateral, contralateral and binaural tone burst stimulation. *Audiology* 1986, 25: 54–61.

Pantev C, Roberts LE, Elbert T, Ross B, and Wienbruch C. Tonotopic organization of the sources of human auditory steady-state responses. *Hear Res* 1996, 101: 62–74.

Pantev C, Ross B, Berg P, Elbert T, and Rockstroh B. Study of the human auditory cortices using a whole-head magnetometer: left vs. right hemisphere and ipsilateral vs. contralateral stimulation. *Audiol Neurootol* 1998, 3: 183–190.

Parkkonen L, Andersson J, Hämäläinen M, and Hari R. Early visual brain areas reflect the percept of an ambiguous scene. *Proc Natl Acad Sci U S A* 2008, 105: 20500–20504.

Parviainen T, Helenius P, and Salmelin R. Cortical differentiation of speech and nonspeech sounds at 100 ms: implications for dyslexia. *Cereb Cortex* 2005, 15: 1054–1063.

Pelizzone M, Hari R, Mäkelä JP, Huttunen J, Ahlfors S, and Hämäläinen M. Cortical origin of middle-latency auditory evoked responses in man. *Neurosci Lett* 1987, 82: 303–307.

Pelizzone M, Kasper A, Hari R, Karhu J, and Montandon P. Bilateral electrical stimulation of a congenitally-deaf ear and of an acquired-deaf ear. *Acta Otolaryngol* 1991, 111: 263–268.

Penhune VB, Zatorre RJ, MacDonald JD, and Evans AC. Interhemispheric anatomical differences in human primary auditory cortex: probabilistic mapping and volume measurement from magnetic resonance scans. *Cereb Cortex* 1996, 6: 661–672.

Peters BR, Wyss J, and Manrique M. Worldwide trends in bilateral cochlear implantation. *Laryngoscope* 2010, 120 Suppl 2: S17–44.

Peterson RL and Pennington BF. Developmental dyslexia. *Lancet* 2012, 379: 1997–2007.

Picton TW, John MS, Dimitrijevic A, and Purcell D. Human auditory steady-state responses. *Int J Audiol* 2003, 42: 177–219.

Pinel P, Fauchereau F, Moreno A, Barbot A, Lathrop M, Zelenika D, Le Bihan D, Poline JB, Bourgeron T, and Dehaene S. Genetic variants of FOXP2 and KIAA0319/TTRAP/THEM2 locus are associated with altered brain activation in distinct language-related regions. *J Neurosci* 2012, 32: 817–825.

Pollack I and Pickett J. Stereophonic listening and speech intelligibility against voice babble. *J Acoust Soc Am* 1958, 30: 131–133.

Purves D, Augustine GJ, Fitzpatrick D, Hall WC, LaMantia AS, McNamara JO, and Williams SM. *Neuroscience*. 2004. Sunderland: Sinauer Associates, Inc.

Rademacher J, Morosan P, Schormann T, Schleicher A, Werner C, Freund HJ, and Zilles K. Probabilistic mapping and volume measurement of human primary auditory cortex. *Neuroimage* 2001, 13: 669–683.

Ramsden JD, Gordon K, Aschendorff A, Borucki L, Bunne M, Burdo S, Garabedian N, Grolman W, Irving R, Lesinski-Schiedat A, Loundon N, Manrique M, Martin J, Raine C, Wouters J, and Papsin BC. European Bilateral Pediatric Cochlear Implant Forum Consensus Statement. *Otol Neurotol* 2012, 33: 561–565.

Rauschecker JP and Tian B. Mechanisms and streams for processing of "what" and "where" in auditory cortex. *Proc Natl Acad Sci U S A* 2000, 97: 11800–11806.

Rauschecker JP, Tian B, Pons T, and Mishkin M. Serial and parallel processing in rhesus monkey auditory cortex. *J Comp Neurol* 1997, 382: 89–103.

Recanzone GH. Perception of auditory signals. *Ann N Y Acad Sci* 2011, 1224: 96–108.

Rees A, Green GG, and Kay RH. Steady-state evoked responses to sinusoidally amplitude-modulated sounds recorded in man. *Hear Res* 1986, 23: 123–133.

Reite M, Edrich J, Zimmerman JT, and Zimmerman JE. Human magnetic auditory evoked fields. *Electroencephalogr Clin Neurophysiol* 1978, 45: 114–117.

Reite M, Zimmerman JT, Edrich J, and Zimmerman JE. Auditory evoked magnetic fields: response amplitude vs. stimulus intensity. *Electroencephalogr Clin Neurophysiol* 1982, 54: 147–152.

Renvall H and Hari R. Auditory cortical responses to speech-like stimuli in dyslexic adults. *J Cogn Neurosci* 2002, 14: 757–768.

Renvall H and Hari R. Diminished auditory mismatch fields in dyslexic adults. *Ann Neurol* 2003, 53: 551–557.

Rivier F and Clarke S. Cytochrome oxidase, acetylcholinesterase, and NADPH-diaphorase staining in human supratemporal and insular cortex: evidence for multiple auditory areas. *Neuroimage* 1997, 6: 288–304.

Rodriguez R, Picton T, Linden D, Hamel G, and Laframboise G. Human auditory steady state responses: effects of intensity and frequency. *Ear Hear* 1986, 7: 300–313.

Romani GL, Williamson SJ, and Kaufman L. Tonotopic organization of the human auditory cortex. *Science* 1982, 216: 1339–1340.

Rosen S. A problem with auditory processing? *Curr Biol* 1999, 9: R698–700.

Rosner T, Kandzia F, Oswald JA, and Janssen T. Hearing threshold estimation using concurrent measurement of distortion product otoacoustic emissions and auditory steady-state responses. *J Acoust Soc Am* 2011, 129: 840–851.

Ross B, Borgmann C, Draganova R, Roberts LE, and Pantev C. A high-precision magnetoencephalographic study of human auditory steady-state responses to amplitude-modulated tones. *J Acoust Soc Am* 2000, 108: 679–691.

Ross J, Tervaniemi M, and Näätänen R. Neural mechanisms of the octave illusion: electrophysiological evidence for central origin. *Neuroreport* 1996, 8: 303–306.

Salminen NH, Tiitinen H, and May PJ. Auditory Spatial Processing in the Human Cortex. *Neuroscientist* 2012.

Sams M and Hari R. Magnetoencephalography in the study of human auditory information processing. *Ann N Y Acad Sci* 1991, 620: 102–117.

Scerri TS and Schulte-Körne G. Genetics of developmental dyslexia. *Eur Child Adolesc Psychiatry* 2010, 19: 179–197.

Scherg M, Hari R, and Hämäläinen M. Frequency-spesific sources of the auditory N10-P30 detected by a multiple source analysis of evoked magnetic fields and potentials. In Williamson SJ, Hoke, M., Stroink, G., Kotani, M. (Ed.) *Advances in Biomagnetism*, 1989. New York: Planum Press, pp. 97–100.

Schnupp J, Nelken I, and King A. *Auditory Neuroscience, Making Sense of Sounds*. 2011. Cambridge, Massachusetts: The MIT Press.

Schulte-Körne G, Deimel W, Bartling J, and Remschmidt H. Speech perception deficit in dyslexic adults as measured by mismatch negativity (MMN). *Int J Psychophysiol* 2001, 40: 77–87.

Scott SK and Johnsrude IS. The neuroanatomical and functional organization of speech perception. *Trends Neurosci* 2003, 26: 100–107.

Shaywitz SE. Dyslexia. *N Engl J Med* 1998, 338: 307–312.

Sigalovsky IS, Fischl B, and Melcher JR. Mapping an intrinsic MR property of gray matter in auditory cortex of living humans: a possible marker for primary cortex and hemispheric differences. *Neuroimage* 2006, 32: 1524–1537.

Snowling M, Bishop DV, and Stothard SE. Is preschool language impairment a risk factor for dyslexia in adolescence? *J Child Psychol Psychiatry* 2000, 41: 587–600.

Stapells DR, Linden D, Suffield JB, Hamel G, and Picton TW. Human auditory steady state potentials. *Ear Hear* 1984, 5: 105–113.

Stein CM, Schick JH, Gerry Taylor H, Shriberg LD, Millard C, Kundtz-Kluge A, Russo K, Minich N, Hansen A, Freebairn LA, Elston RC, Lewis BA, and Iyengar SK. Pleiotropic effects of a chromosome 3 locus on speech-sound disorder and reading. *Am J Hum Genet* 2004, 74: 283–297.

Stein J. The magnocellular theory of developmental dyslexia. *Dyslexia* 2001, 7: 12–36.

Stewart L, von Kriegstein K, Warren JD, and Griffiths TD. Music and the brain: disorders of musical listening. *Brain* 2006, 129: 2533–2553.

Striem-Amit E, Hertz U, and Amedi A. Extensive cochleotopic mapping of human auditory cortical fields obtained with phase-encoding FMRI. *PLoS One* 2011, 6: e17832.

Sweet RA, Dorph-Petersen KA, and Lewis DA. Mapping auditory core, lateral belt, and parabelt cortices in the human superior temporal gyrus. *J Comp Neurol* 2005, 491: 270–289.

Talavage TM, Sereno MI, Melcher JR, Ledden PJ, Rosen BR, and Dale AM. Tonotopic organization in human auditory cortex revealed by progressions of frequency sensitivity. *J Neurophysiol* 2004, 91: 1282–1296.

Tallal P. Improving language and literacy is a matter of time. *Nat Rev Neurosci* 2004, 5: 721–728.

Tarkiainen A, Liljeström M, Seppä M, and Salmelin R. The 3D topography of MEG source localization accuracy: effects of conductor model and noise. *Clin Neurophysiol* 2003, 114: 1977–1992.

Tessier-Lavigne M and Goodman CS. The molecular biology of axon guidance. *Science* 1996, 274: 1123–1133.

Tiihonen J, Hari R, Kaukoranta E, and Kajola M. Interaural interaction in the human auditory cortex. *Audiology* 1989, 28: 37–48.

Tiihonen J, Hari R, Naukkarinen H, Rimon R, Jousmäki V, and Kajola M. Modified activity of the human auditory cortex during auditory hallucinations. *Am J Psychiatry* 1992, 149: 255–257.

Upadhyay J, Ducros M, Knaus TA, Lindgren KA, Silver A, Tager-Flusberg H, and Kim DS. Function and connectivity in human primary auditory cortex: a combined fMRI and DTI study at 3 Tesla. *Cereb Cortex* 2007, 17: 2420–2432.

Wallace MN, Johnston PW, and Palmer AR. Histochemical identification of cortical areas in the auditory region of the human brain. *Exp Brain Res* 2002, 143: 499–508.

van der Zwaag W, Gentile G, Gruetter R, Spierer L, and Clarke S. Where sound position influences sound object representations: a 7-T fMRI study. *Neuroimage* 2011, 54: 1803–1811.

Vartiainen J, Liljeström M, Koskinen M, Renvall H, and Salmelin R. Functional magnetic resonance imaging blood oxygenation level-dependent signal and magnetoencephalography evoked responses yield different neural functionality in reading. *J Neurosci* 2011, 31: 1048–1058.

Vasama JP, Mäkelä JP, Parkkonen L, and Hari R. Auditory cortical responses in humans with congenital unilateral conductive hearing loss. *Hear Res* 1994, 78: 91–97.

Vasama JP, Mäkelä JP, Pyykkö I, and Hari R. Abrupt unilateral deafness modifies function of human auditory pathways. *Neuroreport* 1995, 6: 961–964.

Wessinger CM, VanMeter J, Tian B, Van Lare J, Pekar J, and Rauschecker JP. Hierarchical organization of the human auditory cortex revealed by functional magnetic resonance imaging. *J Cogn Neurosci* 2001, 13: 1–7.

Viceic D, Fornari E, Thiran JP, Maeder PP, Meuli R, Adriani M, and Clarke S. Human auditory belt areas specialized in sound recognition: a functional magnetic resonance imaging study. *Neuroreport* 2006, 17: 1659–1662.

Wilson RH and McArdle R. Speech signals used to evaluate functional status of the auditory system. *J Rehabil Res Dev* 2005, 42: 79–94.

Yost WA. *Fundamentals of Hearing: An Introduction*. 2000. San Diego: Academic Press.

Zhang J, Nakamoto KT, and Kitzes LM. Binaural interaction revisited in the cat primary auditory cortex. *J Neurophysiol* 2004, 91: 101–117.

Zwicker T. Experimente zűr dichotischen Oktav-Tauschung. *Acustica* 1984, 55: 128–136.